

OCEAN DRILLING PROGRAM

LEG 209 SCIENTIFIC PROSPECTUS

**DRILLING MANTLE PERIDOTITE ALONG THE MID-ATLANTIC RIDGE
FROM 14° TO 16°N**

Dr. Peter B. Kelemen
Co-Chief Scientist
Department of Geology and Geophysics
Woods Hole Oceanographic Institution
MS 8
Woods Hole MA 02543
USA

Dr. Eiichi Kikawa
Co-Chief Scientist
Japan Marine Science and
Technology Center
1133 21st Street, Northwest
Suite 400
Washington DC 20036
USA

Dr. Jack Baldauf
Deputy Director of Science Operations
Ocean Drilling Program
Texas A&M University
1000 Discovery Drive
College Station TX 77845-9547
USA

Dr. D. Jay Miller
Leg Project Manager and Staff Scientist
Ocean Drilling Program
Texas A&M University
1000 Discovery Drive
College Station TX 77845-9547
USA

PUBLISHER'S NOTES

Material in this publication may be copied without restraint for library, abstract service, educational, or personal research purposes; however, this source should be appropriately acknowledged.

Ocean Drilling Program Scientific Prospectus No. 109 (November 2002).

Distribution: Electronic copies of this series may be obtained from the ODP Publications homepage on the World Wide Web at <http://www-odp.tamu.edu/publications>.

This publication was prepared by the Ocean Drilling Program, Texas A&M University, as an account of work performed under the international Ocean Drilling Program, which is managed by Joint Oceanographic Institutions, Inc., under contract with the National Science Foundation. Funding for the program is provided by the following agencies:

Australia/Canada/Chinese Taipei/Korea Consortium for Ocean Drilling
Deutsche Forschungsgemeinschaft (Federal Republic of Germany)
European Science Foundation Consortium for Ocean Drilling (Belgium, Denmark, Finland, Iceland, Ireland, Italy, The Netherlands, Norway, Portugal, Spain, Sweden, and Switzerland)
Institut National des Sciences de l'Univers-Centre National de la Recherche Scientifique (INSU-CNRS; France)
Marine High-Technology Bureau of the State Science and Technology Commission of the People's Republic of China
National Science Foundation (United States)
Natural Environment Research Council (United Kingdom)
Ocean Research Institute of the University of Tokyo (Japan)

DISCLAIMER

Any opinions, findings, and conclusions or recommendations expressed in this publication are those of the author(s) and do not necessarily reflect the views of the National Science Foundation, the participating agencies, Joint Oceanographic Institutions, Inc., Texas A&M University, or Texas A&M Research Foundation.

This Scientific Prospectus is based on precruise JOIDES panel discussions and scientific input from the designated Co-chief Scientists on behalf of the drilling proponents. The operational plans within reflect JOIDES Planning Committee and thematic panel priorities. During the course of the cruise, actual site operations may indicate to the Co-chief Scientists and the Operations Manager that it would be scientifically or operationally advantageous to amend the plan detailed in this prospectus. It should be understood that any proposed changes to the plan presented here are contingent upon the approval of the Director of the Ocean Drilling Program in consultation with the Science and Operations Committees (successors to the Planning Committee) and the Pollution Prevention and Safety Panel.

ABSTRACT

Leg 209 of the Ocean Drilling Program will be devoted to coring mantle peridotite along the Mid-Atlantic Ridge (MAR) from 14° to 16°N. This area was identified at the 1996 Workshop on Oceanic Lithosphere and Scientific Drilling into the 21st Century as the ideal region for drilling of a strike line of short holes to sample the upper mantle in a magma-starved portion of a slow-spreading ridge. In this area, igneous crust is locally absent and the structure and composition of the mantle can be determined at sites over ~100 km along strike.

A central paradigm of Ridge Interdisciplinary Global Experiments (RIDGE) program studies is the hypothesis that mantle flow, or melt extraction, or both, are focused in three dimensions toward the centers of magmatic ridge segments, at least at slow-spreading ridges such as the MAR. This hypothesis has essentially reached the status of accepted theory, but it has never been subject to a direct test. A strike line of oriented mantle peridotite samples extending for a significant distance within such magmatic segments offers the possibility of directly testing this hypothesis. Continued dredging and submersible studies cannot provide the spatial information required to make such a test.

The primary aim of drilling is to characterize the spatial variation of mantle deformation patterns, residual peridotite composition, melt migration features, and hydrothermal alteration along axis. Hypotheses for focused solid or liquid upwelling beneath ridge segments make specific predictions regarding the spatial variation of mantle lineation or the distribution of melt migration features. These predictions may be directly tested by drilling.

SITE SURVEY DATA AND OTHER GEOLOGICAL BACKGROUND

The Mid-Atlantic Ridge (MAR) near the 15°20' Fracture Zone (FZ) has been the focus of a long-term cooperative French-American and allied Russian research program. During the summer of 1998 the area was visited by a Japanese/American team, funded in part as a site survey for the Ocean Drilling Program (ODP). In addition to identifying many suitable drill sites, these cruises have completed an extensive shipboard bathymetric, gravity, and magnetics survey over the entire region (Fig. F1). We believe that these data, together with information from submersibles and dredging, have completed the site survey necessary for well-constrained drilling in the region.

In addition to nearly continuous outcrops of mantle peridotite on both walls of the rift valley for at least 100 km from 14°40' to 15°40'N (Fig. F2), significant features of the area include

1. Large "gravity bulls-eyes," concentric, negative residual Bouger and mantle Bouger gravity anomalies, centered at ~14° and 16°N (Fig. F1);
2. A regional chemical anomaly with "hotspot" characteristics, centered at ~14°N (Fig. F3);
3. "Megamullion" structures, interpreted to be long-lived, low-angle faults exposed on the seafloor over regions of ~100 km², for example, at 46°54'W, 15°44'N, (Fig. F2); and
4. At least three areas with high methane signatures in the water column, including one active hydrothermal field within mantle peridotites.

Seismic Studies

In June 1997, a seismic refraction experiment was carried out north of the 15°20' FZ from the *Ewing*, led by John Collins of Woods Hole Oceanographic Institution (WHOI). Using NOBEL (Near Ocean Bottom Explosives Launcher), refraction profiles were shot over areas previously mapped using the submersible

Nautilé. Source and receiver were on the seafloor for determination of seismic velocity structure at length scales of 10 to 100 m, instead of 100 m to 1 km obtained with conventional surveys. The NOBEL profiles were at 15°37'N on (1) an ultramafic outcrop, (2) a gabbro/wehrlite outcrop, and (3) basalt, to determine whether seismic velocities can be used to map the extent of gabbro and peridotite emplaced at or near the seafloor. In addition, a 100-km-long conventional refraction profile was shot along the median valley of the MAR north of the 15°20' FZ. Results show anomalous seismic structure in the crust, with pronounced gradients in velocity, rather than the layered structure typical for fast spreading ridges (Fig. F4). This type of seismic structure is typical for slow-spreading ridges near fracture zones (R. Detrick, pers. comm., 1998).

Submersible Studies

Many possible drill sites were identified during the *Faranaút* cruise with the French *Nautilé* submersible in 1992 (e.g., Cannat et al., 1995, 1997). In 1998, the joint JAMSTEC/WHOI MODE 98, Leg 1 cruise with the Japanese *Shinkai* 6500 submersible completed the survey for possible drill sites. A summary of lithologic observations from dredging and diving is shown in Figure F2, and a summary of proposed drill sites surveyed by submersible is shown in Figure F5. In addition, it is worthy of note that extensive exposures of moderate- to low-angle fault surfaces underlain by peridotite have been observed on the seafloor, particularly at sites MAR-ALT1N and MAR-ALT2S in Figure F5.

Shipboard Geophysics

Although the 1992 *Faranaút* cruise included a shipboard bathymetric, gravity, and magnetics survey, the quality of the gravity and magnetics data was less than optimal. The 1998 MODE 98, Leg 1 cruise conducted additional surveys. The combined *Faranaút* and MODE 98 survey coverage is illustrated in Figure F2 (Cannat et al., 1995, 1997; Casey et al., 1998; Kelemen et al., 1998b; Matsumoto et al., 1998; Fujiwara et al., in press). For the purposes of this scientific prospectus, the most important result is the identification of large “gravity bulls-eyes,” concentric, negative residual Bouger and mantle Bouger gravity anomalies, centered at ~14° and 16°N (Fig. F1). These gravity lows correspond to areas with well-organized seafloor magnetic anomalies and ridge-parallel abyssal hill topography, whereas the relative gravity highs correspond to known areas with outcrop of serpentinized peridotite along the ridge axis and to areas with poorly organized seafloor magnetic anomalies and chaotic topography. Also note that the negative gravity anomaly at 14°N is about twice as large as that at 16°N, in keeping with geochemical indices that the 14°N area resembles a “hotspot” (see “Mantle Temperature and Composition” in “Ancillary Studies”).

The gravity lows are probably centers of magmatic segments where there is accretion of thick igneous crust. The gravity highs are on the periphery of these magmatic segments and therefore are magma starved. This is important because it provides a potential explanation for the extensive outcrops of peridotite along the MAR between 14°40' and 15°40'N. Thus, this region is ideal for testing hypotheses that explain focused crustal accretion along magmatic segments.

Geochemical Background

Extensive analytical work has been done on samples recovered by dredging in the 14° to 16°N region along the MAR (Bonatti et al., 1992; Bougault et al., 1988, 1990; Casey, 1997; Casey et al., 1992, 1994, 1995; Dick and Kelemen, 1992; Dosso et al., 1991; Peyve et al., 1988a, 1988b; Silantyev et al., 1996; Sobolev et al., 1992a, 1992b; Sobolov et al., 1992; Staudacher et al., 1989; Xia et al., 1991, 1992). This work reveals that the mantle source of basalts south of the 15°20'N FZ is geochemically “enriched,” similar

to the source of hotspot-related mid-ocean ridge basalts (MORB) elsewhere along the MAR (Fig. F3). Perhaps related to this is the observation that mantle peridotites seem to have undergone unusually high degrees of melting (mantle olivines have molar Mg/[Mg+Fe] up to 0.92, and spinels have molar Cr/[Cr+Al] up to 0.7, forming the depleted end-members for peridotites recovered from mid-ocean ridges) (Fig. F3). North of the fracture zone, however, basalts and peridotites have compositions typical for the MAR away from hotspots (Fig. F3).

PRIMARY RATIONALE FOR DRILLING

Focused Crustal Accretion at Slow-Spreading Ridges

A central paradigm of Ridge Interdisciplinary Global Experiments (RIDGE) program studies is the hypothesis that mantle flow, or melt extraction, or both, are focused in three dimensions toward the centers of magmatic ridge segments, at least at slow-spreading ridges such as the MAR. This is based on observations from ophiolites, with emphasis on the Oman ophiolite (Ceuleneer, 1991; Ceuleneer et al., 1988; Ceuleneer and Rabinowicz, 1992; Jousset et al., 1998; Nicolas and Boudier, 1995; Nicolas and Rabinowicz, 1984; Nicolas and Violette, 1982), the theory that partially molten mantle may be subject to diapirism via Rayleigh-Taylor instabilities (Barnouin-Jha et al., 1997; Buck and Su, 1989; Crane, 1985; Jha et al., 1994; Parmentier and Phipps Morgan, 1990; Rabinowicz et al., 1984, 1987; Schouten et al., 1985; Sparks and Parmentier, 1993; Sparks et al., 1993; Su and Buck, 1993; Whitehead et al., 1984), the observation that peridotites are commonly dredged near fracture zones along slow-spreading ridges, but not near ridge segment centers (Dick, 1989; Whitehead et al., 1984), and gravity and seismic studies of the MAR suggesting thick crust near segment centers and thin crust at segment ends (e.g., Barclay et al., 1988; Kuo and Forsyth, 1988; Lin et al., 1990; Tolstoy et al., 1993; Tucholke et al., 1997). In addition to the possible role of mantle diapirism, various workers have proposed that melt transport may be focused in two or three dimensions, on the basis of theoretical work and field observations (e.g., Aharonov et al., 1995; Kelemen et al., 1998a, 1995a; Magde et al., 1997; Phipps Morgan, 1987; Sparks and Parmentier, 1991, 1994; Spiegelman, 1993; Spiegelman and McKenzie, 1987). Such focused melt extraction could operate, with or without focused flow of the upwelling mantle, to produce the observed focusing of crustal accretion toward the center of magmatic ridge segments.

The idea that focused mantle upwelling at the centers of magmatic ridge segments occurs only beneath slow-spreading ridges was formulated by Marc Parmentier and his students (e.g., Lin and Phipps Morgan, 1992; Parmentier and Phipps Morgan, 1990; Turcotte and Phipps Morgan, 1992) and is supported by seismic results from the recent Mantle Electromagnetic and Tomography (MELT) experiment along the fast-spreading southern East Pacific Rise, in which no focused mantle upwelling was detected (e.g., Forsyth et al., 1998; Team, 1998; Toomey et al., 1998). However, recent observations from Oman and the fast-spreading northern East Pacific Rise have called this into question (e.g., Barth and Mutter, 1996; Dunn and Toomey, 1997; Nicolas et al., 1996). Nevertheless, most investigators agree that slow-spreading ridges such as the MAR represent the best place to test general hypotheses for the mechanism(s) of three-dimensional focusing of crustal accretion.

Comparison of Models for Mantle Upwelling

In the literature describing theories of three-dimensionally focused mantle upwelling, the terms “focused” and “3-D” receive different definitions from different authors. Thus, Parmentier and Phipps Morgan (1990), who first presented the now-famous “phase diagram” for two-dimensional (2-D) vs. three-

dimensional (3-D) mantle upwelling as a function of spreading rate and mantle viscosity, chose a detailed example that is indeed 3-D but that does not correspond well to observations of diapirs in the mantle section of the Oman ophiolite. In Parmentier and Phipps Morgan's (1990) example, the region of mantle upwelling at, for example, 40 km depth is ~200 km wide in a ridge-parallel section and widens upward; near the top it is almost as wide as their 300-km ridge segment. Along-ridge transport of upwelling mantle occurs gradually over the upper 60 km of the upwelling region.

In contrast, the interpretation of Joussetin et al. (1998), loosely based on observations from Oman, is that "at any depth above 50 km there is no vertical flow outside the narrow zone of subridge upwelling." They take the zone of upwelling to be cylindrical, with a diameter of ~10 km. Furthermore, in their interpretation, all corner flow (ridge parallel and ridge perpendicular) occurs in the upper 500 m of the upwelling region. More than half of the shallow mantle in their 25-km-long ridge segments is fed by horizontal flow in this 500-m-thick layer just below the base of the lithosphere. Such narrow pipes of upwelling mantle may be consistent with the physical models of Buck and Su (1989) (Su and Buck, 1993), which show very sharp focusing of mantle flow. Such features could conceivably have escaped seismic detection in the recent MELT experiment. However, if this is the geometry of mantle upwelling, then the amount of ridge-parallel horizontal transport of mantle material must be very large.

In the ensuing discussion, we take the Joussetin et al. (1998) geometry as the end-member example of 3-D focused mantle flow and passive corner flow to be the end-member example of 2-D mantle flow with no focusing. The Joussetin et al. (1998) scenario may seem extreme at first, but it does provide a clear description of an upwelling geometry that could produce a variation in igneous crustal thickness from ~10 km at a segment center to ~0 km near the segment ends, as interpreted on the basis of geological and geophysical observations in the 14° to 16°N region of the MAR. These observations are typical of the first-order features of slow-spreading ridges, which are thought to reflect three-dimensionally focused magmatic accretion.

In contrast, available 3-D physical models of diapiric mantle upwelling beneath ridges cannot account for these observations because the upwelling is not sufficiently tightly focused. As stated by Barnouin-Jha et al. (1997), "short wavelength segmentation of slow spreading centers requires some process not included in our models of mantle flow." This missing process might be tightly focused upwelling, as in the scheme of Joussetin et al. (1998) or focused melt migration.

Testing Hypotheses for the Mechanism(s) of Focused Crustal Accretion

Despite the difficulties with 3-D physical models, outlined in the previous section, the hypothesis that mantle flow, or melt extraction, or both, are focused in three dimensions toward centers of magmatic segments at slow-spreading ridges has essentially reached the status of accepted theory. However, these ideas have never been subject to a direct test. A strike line of oriented mantle peridotite samples extending for a significant distance within such magmatic segments offers the possibility of directly testing hypotheses for focused crustal accretion.

The primary aim of drilling in the 14° to 16°N area along the MAR is to characterize the spatial variation of mantle deformation patterns, residual peridotite composition, melt migration features, and hydrothermal alteration along axis. Published hypotheses for focused solid or liquid upwelling beneath ridge segments make specific predictions regarding the spatial variation of mantle lineation or the distribution of melt migration features, which can be tested by drilling.

Interpretation of Ductile Flow Fabrics in Mantle Peridotites

Models of focused solid upwelling require ridge-parallel, subhorizontal flow of residual mantle peridotites from segment centers to segment ends (Fig. F6A) (Barnouin-Jha et al., 1997; Buck and Su, 1989; Crane, 1985; Jha et al., 1994; Parmentier and Phipps Morgan, 1990; Rabinowicz et al., 1984, 1987; Schouten et al., 1985; Sparks and Parmentier, 1993; Sparks et al., 1993; Su and Buck, 1993; Whitehead et al., 1984). This is supported to some extent by patterns of mantle flow inferred from ductile fabrics in residual peridotites in the Oman ophiolite (Fig. F6B) (Ceuleneer et al., 1998; Ceuleneer et al., 1991; Ceuleneer and Rabinowicz, 1992; Jousset et al., 1998; Nicolas and Boudier, 1995; Nicolas and Rabinowicz, 1984; Nicolas and Violette, 1982), although, as already noted previously, the scale of focused upwelling in Oman (~10 km) is different from that in current 3-D models of mantle diapirism (~100 km). Mantle flow direction may be determined by measurement of spinel shape fabrics (lineation at high strain is parallel to ductile flow), measurement of the orientation of olivine crystal shape fabrics relative to subgrain boundaries (subgrain boundaries are oblique to the long sides of elongate crystals, indicating the sense of shear), and measurement of olivine crystal lattice preferred orientation (olivine a-axes are aligned parallel to ductile flow directions at high strain).

Cores from a series of drill holes in mantle peridotite along a slow-spreading ridge axis can, in principle, be used to test the prediction that shallow ductile flow of residual mantle at the ends of segments is ridge-parallel and subhorizontal. There are two problems with this approach: (1) the core must be restored to a geographical reference frame, and (2) tectonic rotations of the peridotite that postdate ductile flow must be considered before the orientation of ductile fabrics can be interpreted in terms of large-scale mantle flow. Work on cores of partially serpentinized mantle peridotite from the East Pacific (Boudier et al., 1996) and the Atlantic (Ceuleneer and Cannat, 1997) have shown that they can be reoriented into the geographical reference frame using remanent magnetization (Hurst et al., 1997; Kelso et al., 1996; Kikawa et al., 1996; Lawrence et al., 1997; Richter et al., 1996). Where the magnetic inclination in the core after horizontal rotation is not parallel to the inferred magnetic inclination at the time of lithospheric formation, tectonic rotations may be inferred and then "removed." However, an important caveat is that the remnant magnetization in partially serpentinized peridotites is hosted in magnetite that is produced during serpentinization, so that tectonic rotations of the peridotite prior to serpentinization cannot be detected.

Accounting fully for possible tectonic rotations of exposed mantle peridotite is a daunting prospect, but there is hope for a definitive result for the following reasons. Magnetic susceptibility anisotropy data also may provide information about the tectonic stress field where magnetite grains become aligned following serpentinization. Tectonic rotations resulting from normal faults are likely to occur mainly around axes parallel to the ridge axis. Thus, subhorizontal ridge-parallel flow lineation is likely to be affected very little, if at all. Furthermore, rotations are likely to be away from the ridge axis, increasing the angle between lineations and the ridge axis. Thus, if ridge-parallel lineations are consistently observed, this can be taken as good evidence that shallow ductile flow of the mantle was indeed parallel to the ridge. In the best case, observation of systematically varying ductile flow lineations in mantle peridotite, ranging from nearly ridge-perpendicular lineation near segment centers to ridge-parallel lineations near segment ends could be taken as very strong evidence that focused mantle upwelling did occur near segment centers.

Interpretation of Chemical Variation in Mantle Peridotites

Models of focused crustal accretion predict different patterns of mantle depletion resulting from melt extraction as a function of distance from magmatic segment centers. For strongly focused 3-D mantle

flow, there should be no variation in the degree of mantle depletion along axis, since all of the shallow mantle peridotites originate within a narrow, pipelike upwelling zone. For purely passive corner flow, with no other factors considered, again there should be no variation in depletion along axis. However, when passive flow is coupled with cooling of the ends of ridge segments against a fracture zone wall, then the degree of melting is predicted to decrease along axis away from segment centers. This has been termed the “transform edge effect” (Ghose et al., 1996; Langmuir and Bender, 1984; Magde et al., 1997; Phipps Morgan and Forsyth, 1988). Provided that melt extraction is equally efficient throughout the melting region, this variation in melt production should be observed in shallow mantle samples. If partial crystallization of melt migrating into conductively cooled mantle lithosphere occurs, forming “impregnated peridotites” (e.g., Ceuleneer et al., 1988; Ceuleneer and Rabinowicz, 1992; Dick, 1989; Elthon et al., 1992; Seyler and Bonatti, 1997), then this should occur primarily near fracture zones, enhancing the chemical signal of the transform edge effect in mantle peridotites. Furthermore, impregnated peridotites often preserve structural relationships indicative of the nature of melt migration. Impregnated peridotite samples from the western ridge-transform intersection (RTI) of the Kane Fracture Zone (Ishizuka et al., 1995) show evidence for migration of melts into localized ductile shear zones, suggesting that melt migration extended into the active transform fault.

In general, geochemists have searched for the transform edge effect in lavas, which is complicated by the difficulties of seeing through variations in crustal differentiation processes and mantle source composition. Detailed analysis of a suite of peridotite samples, collected from a single ridge segment at various distances from a fracture zone, could provide an independent evaluation of the presence and importance of the transform edge effect.

Interpretation of Melt Transport Features in Mantle Peridotites

Models of focused melt migration toward ridge segment centers predict various different spatial distributions and orientations of melt transport features. Before discussing the various predictions, we will introduce some of the melt transport features that can be recognized in mantle peridotite samples. For reviews of the literature on these features, please see papers by Nicolas (1986, 1990) and Kelemen et al. (1997, 1995a).

1. Dunites are rocks composed almost entirely of the mineral olivine, with minor spinel; pyroxene generally forms <1% of these rocks. Dunites are present in tabular to cylindrical bodies in ophiolite peridotites. Few, if any, are tabular dikes filled entirely with magmatic olivine. Instead, most or all form by dissolution of pyroxene and crystallization of a smaller amount of olivine in olivine-saturated melt migrating by porous flow. Some have an origin entirely via focused porous flow, either in dissolution channels or within ductile shear zones, whereas others form in porous reaction zones around cracks. The relative importance of entirely porous vs. fracture-related origins for dunites is controversial but is not crucial to this science plan. The main point to be made here is that dunites commonly form in the region of adiabatic mantle upwelling beneath spreading ridges, though they also form within the region of transition between adiabatic upwelling and conductively cooled lithosphere.
2. Pyroxenite and gabbro mantle dikes are highly elongate, generally parallel-sided features that almost certainly form as fracture-filling magmatic rocks. Their compositions, where they have been studied in detail, are indicative of crystal fractionation from magma that was cooling within conductive “lithosphere.” However, this is debated, and Nicolas and co-workers have interpreted

them to be representative of melt-filled fractures that form within the adiabatically upwelling mantle.

We now consider predictions of spatial distribution and orientation of melt migration features, with an emphasis on dunites formed within the adiabatically upwelling mantle. Most models predict that such dunites are transposed into a subhorizontal orientation in the shallow mantle, at least by 2-D corner flow and perhaps also by 3-D diapiric flow (dunites that are not subhorizontal may have formed in the region of transition from adiabatically upwelling mantle to conductively cooled lithosphere).

1. If melt migration and crustal accretion are focused mainly because of diapirism, as proposed by Nicolas (1990), then no systematic variation in dunite abundance along the ridge axis is predicted. Furthermore, if melt-filled fractures form within mantle diapirs and these are represented by mantle dikes (Nicolas, 1990), then mantle dikes may be nearly vertical near segment centers and progressively transposed into a horizontal orientation toward segment ends.
2. If melt migration and crustal accretion are focused mainly because of melt migration beneath permeability barriers parallel to the base of the lithosphere, as proposed by Sparks and co-workers (Magde et al., 1997; Sparks and Parmentier, 1991, 1994) and Spiegelman (1993), then dunites should be shallowest (and most commonly sampled by drilling) near the centers of segments.
3. If melt migration and crustal accretion are focused mainly as a result of coalescing porous flow within the upwelling mantle, as proposed by Phipps Morgan (1987), Spiegelman and McKenzie (1987), Kelemen and co-workers (Aharonov et al., 1995; Kelemen et al., 1995a, 1995b, 1998a), and Daines, Zimmerman, and Kohlstedt (Daines and Kohlstedt, 1997; Kohlstedt and Zimmerman, 1996), then dunite abundance in the shallow mantle should increase toward segment centers. Thus, if porous flow mechanisms predominate in producing focused crustal accretion, then dunite abundance should increase toward segment centers, whereas if diapiric upwelling is the predominant reason for focused crustal accretion, then dunite abundance should be relatively constant along axis.

On a smaller scale, the detailed size/frequency and spatial distribution statistics of a large number of dunite veins in outcrops of mantle peridotite can be used as indicators of the geometry of melt extraction conduits (Kelemen et al., 1998a, Braun and Kelemen, in press). Dunites in mantle outcrops in the Ingalls and Oman ophiolite show a negative power-law relationship between size and abundance, with many small dunites and only a few large ones. This is consistent with the hypothesis that dunites form an interconnected channel network, in which many small conduits feed a few large ones. We hope that the systematics of the spatial distribution can be used to distinguish between dunites that originate as reaction zones around cracks and dunites that form entirely as a result of porous flow mechanisms. Drill core samples are ideal for this type of study, which would be a secondary goal of the proposed drilling in the 14° to 16°N area.

ANCILLARY STUDIES

Mantle Temperature and Composition

Along the MAR near Iceland and the Azores, major element indices of the degree of mantle melting (Na/Mg in lavas and pyroxene content in peridotites) suggest an unusually high degree of melting, if one assumes constant source composition. In contrast, trace element indices (high La/Sm or K/Ti) from the

same regions, interpreted in the same way, indicate a small degree of melting. This apparent paradox is easily resolved; the mantle source composition is not constant along the ridge (e.g., Schilling, 1973). This is borne out by radiogenic isotope ratios, which indicate a long-term enrichment in incompatible elements (such as La and K) in the mantle source where the degree of melting is large (e.g., Hart et al., 1973). Enriched areas with apparent high degrees of melting areas have been interpreted as “hotspots,” in accord with the notion that high temperature and chemical enrichment are correlated in the mantle. However, because this correlation between temperature and enrichment is poorly understood and may vary from place to place, there is debate over their relative importance in controlling igneous crustal thickness, crustal composition, axial depth, and geoid height.

Work in the 14° to 16°N region along the MAR can provide constraints for deconvolving the effects of temperature and composition on mantle melting. There is a substantial gradient over 150 km along the ridge, from geochemically “normal” MORB in the north (moderately high Na/Mg and low La/Sm) to strongly “enriched” MORB in the south (low Na/Mg and high La/Sm) (Fig. F3), there is a large gradient in crustal thickness, increasing away from the fracture zone. One hypothesis holds that “enriched” basalts are derived by partial melting of veins that comprise a few percent of the volume of the source region. Drill core will provide a sample that permits determination of the proportion of volumetrically minor veins in the peridotite, and isotope measurements on these veins may place constraints on the original composition of these veins prior to decompression melting.

Hydrothermal Alteration of Peridotite Outcrops

Another goal of drilling will be characterization of hydrothermal alteration of mantle peridotite and plutonic rocks to quantify chemical changes associated with alteration of peridotite at a variety of temperatures. Systematic geochemical studies of samples with a variety of different extents and types of alteration is necessary to discriminate between trace element features retained from igneous processes vs. those that are dominantly imposed during open system alteration. It is now recognized that a large proportion of slow-spreading lithosphere is composed of serpentinized peridotite, which is eventually subducted, but the composition of this geochemical reservoir is poorly characterized and understood. Also, as for melt transport veins, discussed above, continuous core can be used for detailed studies of the size/frequency and spatial distribution statistics of alteration veins, providing important information on the mechanisms of vein formation and fluid transport (e.g., Kelemen et al., 1998a; Magde et al., 1995).

Crustal Thickness Variations and Gabbro Plutons in Peridotite

A variety of recent observations on slow-spreading ridges including the MAR suggests that the crust in these settings is a complicated mixture of gabbroic plutons and partially serpentinized peridotite (review in Cannat, 1996). Mantle peridotite is known to crop out along both flanks of the MAR from at least 14°40' to 15°40'N (Fig. F2). In some cases, lava flows lie directly over mantle peridotite without intervening gabbroic “lower crust.” Thus, this region is “magma-starved,” an end-member compared to the “robust” East Pacific Rise.

Surprisingly, seismic surveys of regions of slow-spreading ridges with abundant peridotite outcrops generally yield significant crustal thicknesses, if crust is defined as material with a seismic *P*-wave velocity of <8 km/s. This is true, for example, for the MAR just north of the 15°20'N FZ, within the proposed drilling area (Fig. F4) (R. Detrick and J. Collins, pers. comm., 1998). In general, seismic data have been used to determine an average crustal thickness of 6 to 7 km for oceanic crust formed far from mantle

hotspots, independent of spreading rate (e.g., White et al., 1992). This paradox represents a first-order problem in studies of the global ridge system.

If possible, it will be very important to develop a geophysical technique for distinguishing between partially serpentinized peridotite and plutonic gabbroic rocks, even where these have the same seismic velocity and density (e.g., Christensen and Salisbury, 1975; Miller and Christensen, 1997). Obtaining extensive drill core of altered mantle peridotite from well below the surface weathering horizon in the 15°N area, together with prior geophysical characterization of this area and downhole logging, will be a first step in resolving this problem. Physical properties of the samples measured in the laboratory (remnant magnetization, density, seismic velocities and attenuation, and electrical conductivity) can be compared with geophysical data in order to calibrate the large-scale surface techniques used worldwide. Some of these physical properties are likely to be scale dependent, so that in addition to downhole geophysical logging, we suggest that a second ship be used, at a later time, to conduct seismic and electrical conductivity experiments using downhole instruments and seafloor sources. A combination of lithologic observations on core and geophysical measurements made at true seismic wavelengths can then be used to seek out features in the geophysical signals that are characteristic of partially serpentinized peridotite and truly measurable in the field.

Nature and Source of Magnetization in Serpentinized Peridotites

Although serpentinized peridotite may comprise a significant proportion of slow-spreading lithosphere, extending up to the seafloor, regional geophysical surveys show a systematic alternation of normal and reversed magnetized seafloor correlated with crustal age, just as in fast-spreading volcanic Pacific crust. Although our drilling leg will not focus on this problem, we will obtain substantial data on the magnetic properties of serpentinized peridotite, which will aid in interpretation of magnetic data for crust formed at slow-spreading ridges.

DRILLING STRATEGY

Although core recovery is our ultimate operational objective, we recognize that bare rock borehole initiation and hard rock coring typically yield recovery of <50%. We hope to improve our recovery by retrieving core barrels after cutting nominally 4.75 m of core (half cores). Although this doubles the amount of time spent in wireline trips, thus reducing time in coring operations, it has coaxed higher recovery from challenging formations. We also intend to employ chrome-lined core barrels (to reduce friction on entry of the core into the core barrel), as data indicate recovery in serpentinized peridotite at Site 920 was significantly (~15%) improved when using chrome-lined core barrels.

At each drill site, the objective will be to core as deeply as operational constraints allow on single bit penetrations into mantle peridotite with a nominal target of recovering >100 m of core. Implementing extended bottom-hole assembly (BHA) configurations, we expect the limit of penetration to generally be ~200 meters below seafloor (mbsf). If conditions allow and scientific objectives warrant, we can envision utilizing operational time at one or more sites to core to greater depths (as deep as 300 mbsf). Our ideal strategy will be to core to bit destruction on our first borehole attempt, to release the bit in the bottom of the hole via a mechanical bit release, and to complete two wireline logging runs through the open pipe (see "Downhole Measurements Plan"). In the event initial penetration is limited or recovery is low, we may opt to attempt additional penetrations as time allows.

Primary Drilling Targets

We have identified seven primary and four alternate drill sites. We do not intend to occupy any of the alternate sites in lieu of our primary sites. However, if operations at primary targets produce unsatisfactory results or to enhance the results of the expedition if time remains after occupation of all primary sites, we may choose to occupy one or more alternate site. All of the primary sites are on the western wall of the rift valley within 10 km of the ridge axis, have been visited by submersible, have a low slope angle, and are thought to be underlain by partially serpentinized mantle peridotite on the basis of geological observations and submersible sampling. Three of the primary sites are north of the 15°20'N FZ, and four are south of the fracture zone. Our operational plan (see Table T1) includes time for coring and logging at each of the seven primary sites. However, to allow for unanticipated time loss, we expect to occupy only three of the southern sites then transit and occupy the three northern sites, before returning for operations at the fourth of the southern sites, as time allows.

Specific Site Objectives

Prospectus Sites MAR-1N, MAR-2N, and MAR-3N

This transect of three sites on the west wall of the MAR rift valley will sample serpentinized peridotite from near the ridge segment center, at an intermediate position between the segment center and the 15°20'N Fracture Zone, and at an exposure of peridotite near the segment end.

Prospectus Sites MAR-1S, MAR-2S, MAR-3S, and MAR-4S

This transect of four sites on the west wall of the MAR rift valley will sample serpentinized peridotite on the inside corner high, to intermediate locations with some gabbroic outcrops identified, and toward the segment center near 14°N.

Alternate Drilling Targets

Prospectus Site MAR-ALT1N

This site is located on the summit of a “megamullion” structure, interpreted as a low-angle normal fault surface exposed on the seafloor for ~100 km². The site is >20 km off axis and in shallow water. It is underlain by a mixture of gabbroic rocks, dunites, and residual mantle peridotites. This is also the farthest north site in the region from which peridotite samples have been recovered. At the time of prospectus preparation, Site MAR-ALT1N is deemed our highest-priority alternate site.

Prospectus Site MAR-ALT2N

This site is located on a small topographic dome within a broad part of the axial valley. It was also the site of one of the NOBEL seismic experiments in 1997. Results of these experiments are still being interpreted. If it is determined on the basis of the NOBEL results to be a place where unaltered or only slightly serpentinized peridotite is <200 mbsf, then this site would become a high-priority drilling target.

Prospectus Site MAR-ALT1S

This is the shallowest point in the region, at only 1650 m below sea level. Four dredge hauls from all sides of this mountain recovered peridotite. Part of the transverse ridge mountains, with a fairly flat top, this site has the potential to be similar to Site 735, but for mantle drilling.

Prospectus Site MAR-ALT2S

This site is located on the ridge at the eastern limit of the axial valley. Dive 425 was underlain almost entirely by a single exposed fault surface of mylonitic peridotite. This site is on the flat-topped ridge above

this fault surface, and drilling is likely to penetrate the footwall of the observed low-angle fault. This is also the farthest south site in the region from which peridotite has been sampled.

SAMPLING PLAN

The ODP Sample Distribution, Data Distribution, and Publications Policy is posted at <http://www-odp.tamu.edu/publications/policy.html>. The Sample Allocation Committee (SAC), which consists of the two co-chief scientists, the staff scientist, the ODP onshore curator, and the curatorial representative onboard ship, will work with the entire science party to formulate a formal Leg 209-specific sampling plan for shipboard and postcruise sampling.

Shipboard scientists are expected to submit sample requests (<http://www-odp.tamu.edu/curation/subsfrm.htm>) no later than 3 months before the beginning of the cruise (by early February 2003). Based on sample requests (shore based and shipboard) submitted by this deadline, the SAC will prepare a tentative sampling plan, which will be revised on the ship as dictated by recovery and cruise objectives. The sampling plan will be subject to modification depending upon the actual material recovered and collaborations that may evolve between scientists during the leg.

Based on the results of coring serpentized peridotite during Leg 153, we expect to recover at least 500 m of core. The minimum permanent archive will be the standard archive half of each core. Samples for shipboard studies will be collected routinely (likely daily) following core labeling, nondestructive whole-core measurements (multisensor track measurements and possibly whole-core images), core splitting, description and close-up photography of intervals of interest, and core description. Shipboard samples for geochemical, mineralogical, and fabric analyses and for physical properties measurements will be extracted from working halves of cores by the shipboard party. When possible, our goal will be to make as many measurements as possible on common samples, thus reducing the amount of material removed from the core and enhancing the opportunity for data correlation.

We expect sampling for postcruise research to take place at sporadic intervals during the expedition (as opposed to routine daily sampling) when sufficient core has been recovered to allow scientists to formulate a circumspect sampling strategy. All personal sample frequencies and sample volumes taken from the working half of the core must be justified on a scientific basis and will be dependent on core recovery, the full spectrum of other requests, and the cruise objectives. Historically, requesting scientists could expect to receive nominally 100 samples of no more than 15 cm³. Postcruise research projects that require more frequent sampling or larger sample volumes should be justified in sample requests. Some redundancy of measurement is unavoidable, but minimizing redundancy of measurements among the shipboard party and identified shore-based collaborators will be a factor in evaluating sample requests.

If some critical intervals are recovered (e.g., fault gouge, veins, fresh peridotite, gabbroic intervals, melt lenses, etc.), there may be considerable demand for samples from a limited amount of cored material. These intervals may require special handling, a higher sampling density, reduced sampling size, or continuous core sampling by a single investigator. A sampling plan coordinated by the SAC may be required before critical intervals are sampled.

DOWNHOLE MEASUREMENTS PLAN

Our logging strategy for Leg 209 is designed to directly complement and/or complete our overall cruise objectives, determining the orientation of deformation fabrics with respect to the Mid-Atlantic Ridge axis and the proportions and orientation of melt features. Downhole logging may, in fact, provide our only continuous record because of the potential of low core recovery. Because of its potential impact on

achieving cruise objectives, we have scheduled time for downhole logging operations at all seven primary sites. We expect our penetration depth to be limited (<200 mbsf) by single bit holes, BHA configurations, and formation instability, so our specific logging strategy will be dictated by contribution to the overall science objectives. The main objectives of the wireline logging program will be to orient faults, fractures, and deformation features using borehole imaging techniques. Borehole images may then help orient core pieces or sections if the core recovery is sufficiently high. In addition to defining structural features, the logging program will also attempt to establish lithologic boundaries as interpreted from logging tool response characteristics as a function of depth, determine serpentinization and/or alteration patterns in lower crustal and upper mantle rocks that might be encountered, and produce direct correlations with discrete laboratory measurements on the recovered core. As with our drilling strategy, the logging program will be determined on a site-by-site basis, through coordination between co-chief scientists, the logging staff scientist, the operations manager, and the staff scientist.

Potential complications in determining the orientation of structural features using downhole imaging techniques may arise from the effect of highly magnetized formations on the three-component magnetometer of the General Purpose Inclinerometry Tool (GPIT), which is the tool used for orienting the images produced by the Formation MicroScanner (FMS). Results from shipboard paleomagnetic studies and the GPIT will be compared in order to assess variations in orientation resulting from high formation magnetization intensities. Hole stability and time constraints will also dictate the amount of wireline logging completed during Leg 209.

Projected Wireline Logging Plan

If hole stability and/or time constraints are not an issue, single-bit holes will be drilled to bit destruction, the bit will be released at the bottom of the hole, and the deepest hole in each site will be logged. This process will not require hole reentry procedures, and time estimates for logging operations are shown below not including time estimates for hole preparation that are included in the operations plan. Time estimates and planned wireline logging tool strings are listed in Table T2.

A wireline logging program has been designed for logging the seven main targets using the triple combination (triple combo) and FMS/sonic tool strings. The triple combo tool string will be used to determine concentrations of K, U, and Th, obtain formation density, measure photoelectric effect, electrical resistivity, and porosity values, and determine borehole conditions. These measurements will be utilized for the characterization of stratigraphic sequences, the assessment of variations in serpentinization, and the identification of oxide mineral-rich intervals. If lithologies with different proportions of ferromagnesian phases (i.e., dunite and harzburgite) manifest different degrees of serpentinization over short intervals, then combinations of density and other logging data might prove useful in distinguishing between them and determining formation thicknesses.

The FMS will provide high-resolution borehole images of stratigraphic sequences and boundaries, oriented fracture patterns, fracture apertures, fracture densities, and information regarding hole stability. The Dipole Sonic Imager (DSI) will produce a full set of compressional and shear waveforms that can be used to determine the nature of the shallow velocity gradient in this area. Cross-dipole shear wave velocities measured at different azimuths may be used to determine preferred mineral, fracture, and/or fabric orientations that may produce seismic velocity anisotropy.

Logging While Coring

Historically, wireline logging programs have met with limited success in hard rock coring expeditions (e.g., Gillis, Mével, Allan, et al., 1993; Cannat, Karson, Miller, et al., 1995). In anticipation of challenging coring and wireline operations, the resistivity-at-the-bit tool with coring capabilities (RAB-C) will likely be substituted for conventional coring and/or logging at selected sites. The strategy for using the RAB-C will be determined on the basis of the ability to obtain wireline logs at a particular site, and the frequency of its use will be determined depending on the amount of core recovered.

The RAB-C will provide borehole resistivity logs and images at three different depths of investigation, total gamma ray logs, and coring capabilities. This tool was first used by ODP during Leg 204 and has the capabilities of recovering 2.56-in (6.5 mm) diameter cores. The RAB-C also provides complete azimuthal coverage of the borehole, providing high-quality resistivity images comparable to those obtained with the FMS. These data will provide visual recognition of igneous layers as well as the identification of fracture patterns, structural orientations, and formation thicknesses. In the past, core recovery has been low in the upper 50 m of holes drilled with conventional drilling techniques (i.e., Legs 147 and 153), and wireline logging techniques preclude the acquisition of downhole measurements at shallow depths because of the need to have the BHA several tens of meters inside the hole. Therefore, the RAB-C data will also provide the only means to obtain continuous information in the upper sections of the holes drilled during Leg 209.

If all or most holes can be logged with conventional wireline techniques, the RAB-C will be used for drilling the last hole during the cruise to determine the tool capabilities in a hard rock environment. The conventional RAB tool without coring capability will be on board as an ultimate backup device.

REFERENCES

- Aharonov, E., Whitehead, J.A., Kelemen, P.B., and Spiegelman, M., 1995. Channeling instability of upwelling melt in the mantle. *J. Geophys. Res.*, 100:20433–20450.
- Barclay, A.H., Toomey, D.R., and Solomon, S.C., 1988. Seismic structure and crustal magmatism at the Mid-Atlantic Ridge, 35°N. *J. Geophys. Res.*, 103:17827–17844.
- Barnouin-Jha, K., Parmentier, E.M., and Sparks, D.W., 1997. Buoyant mantle upwelling and crustal production at oceanic spreading centers; on-axis segmentation and off-axis melting. *J. Geophys. Res.*, 102:11979–11989.
- Barth, G.A., and Mutter, J.C., 1996. Variability in oceanic crustal thickness and structure: multichannel seismic reflection results from the northern East Pacific Rise. *J. Geophys. Res.*, 101:17951–17975.
- Bonatti, E., Peyve, A., Kepezhinskas, P., Kurentsova, N., Seyler, M., Skolotnev, S., and Udintsev, G., 1992. Upper mantle heterogeneity below the Mid-Atlantic Ridge, 0°–15°N. *J. Geophys. Res.*, 97:4461–4476.
- Boudier, F., MacLeod, C.J., and Bolou, L., 1996. Structures in peridotites from Site 895, Hess Deep: implications for the geometry of mantle flow beneath the East Pacific Rise. In Mével, C., Gillis, K.M., Allan, J.F., and Meyer, P.S. (Eds.), *Proc. ODP, Sci. Results*, 147: College Station, TX (Ocean Drilling Program), 347–356.
- Bougault, H., Dmitriev, L., Schilling, J.G., Sobolev, A., Joron, J.L., and Needham, H.D., 1988. Mantle heterogeneity from trace elements: MAR triple junction near 14°N. *Earth Planet. Sci. Lett.*, 88:27–36.
- Bougault, H., and others, 1990. Campagne RIDELENTE: Structure de la dorsale Atlantique Heterogeniete du manteau et hydrothermalisme, *Oceanologica Acta* (special issue), 10:366–381.
- Braun, M.G., and Kelemen, P.B., in press. Dunite distribution in the Oman ophiolite: implications for melt flux through porous dunite conduits. *Geochem., Geophys., Geosys.*
- Buck, W.R., and Su, W., 1989. Focused mantle upwelling below mid-ocean ridges due to feedback between viscosity and melting. *Geophys. Res. Lett.*, 16:641–644.
- Cannat, M., 1996. How thick is the magmatic crust at slow-spreading oceanic ridges? *J. Geophys. Res.*, 101:2847–2857.
- Cannat, M., Karson, J.A., Miller, D.J., et al., 1995. *Proc. ODP, Init. Repts.*, 153: College Station, TX (Ocean Drilling Program).
- Cannat, M., Lagabriele, Y., Bougault, H., Casey, J., de Coutures, N., Dmitriev, L., and Fouquet, Y., 1997. Ultramafic and gabbroic exposures at the Mid-Atlantic Ridge: geological mapping in the 15 degrees N region. *Tectonophysics*.
- Cannat, M., Mével, C., Maia, M., Deplus, C., Durand, C., Gente, P., Agrinier, P., Belarouchi, A., Dubuisson, G., et al., 1995. Thin crust, ultramafic exposures, and rugged faulting patterns at the Mid-Atlantic Ridge (22°–24°N). *Geology*, 23:49–52.
- Casey, J.F., 1997. Comparison of major- and trace-element geochemistry of abyssal peridotites and mafic plutonic rocks with basalts from the MARK region of the Mid-Atlantic Ridge. In Karson, J.A., Cannat, M., Miller, D.J., and Elthon, D. (Eds.), *Proc. ODP, Sci. Results*, 153: College Station, TX (Ocean Drilling Program), 181–241.

- Casey, J.F., Braun, M., Kelemen, P.B., Fujiwara, T., Matsumoto, T. and Shipboard Scientific Party, 1998. Megamullions along the Mid-Atlantic Ridge between 14° and 16°N: results of Leg 1, JAMSTEC/WHOI MODE 98 Survey. *Eos*, 79:F920.
- Casey, J.F., Bryan, W.B., Xia, C., Smith, S., Dmitriev, L., Silantiev, S., and Melson, W.G., 1992. Basalt compositional trends, 12° to 38°N along the Mid-Atlantic Ridge: local paradigms. *Eos*, 73:584.
- Casey, J.F., Bryan, W.F., and Silantiev, S., 1994. Comparison of the geochemistry of basaltic, plutonic and residual mantle rocks from the Mid-Atlantic Ridge: evidence of near fractional melting and mixing. *Eos*, 75:657.
- Casey, J.F., Smith, S.E., Bryan, W.B., and Silantiev, S., 1995. Major and trace element geochemistry of basalts, gabbros, and peridotites from the northern MAR: an assessment of the range of subaxial parental and evolved melt compositions. *Eos*, 76:694.
- Ceuleneer, G., 1991. Evidences for a paleo-spreading center in the Oman ophiolite: mantle structures in the Maqсад area. In Peters, T., Nicolas, A., and Coleman, R.G. (Eds.), *Ophiolite Genesis and Evolution of Oceanic Lithosphere*: Dordrecht (Kluwer), 147–173.
- Ceuleneer, G., and Cannat, M., 1997. High-temperature ductile deformation of Site 920 peridotites. In Karson, J.A., Cannat, M., Miller, D.J., and Elthon, D. (Eds.), *Proc. ODP, Sci. Results*, 153: College Station, TX (Ocean Drilling Program), 23–34.
- Ceuleneer, G., Nicolas, A., and Boudier, F., 1988. Mantle flow patterns at an oceanic spreading centre: the Oman peridotite record. *Tectonophysics*, 151:1–26.
- Ceuleneer, G., and Rabinowicz, M., 1992. Mantle flow and melt migration beneath ocean ridges: models derived from observations in ophiolites. In Phipps Morgan, J.B., Blackman, D.K., and Sinton, J.M. (Eds.), *Mantle Flow and Melt Generation at Mid-Ocean Ridges*. Geophys. Monogr., Am. Geophys. Union, 71:123–154.
- Christensen, N.I., and Salisbury, M.H., 1975. Structure and constitution of the lower oceanic crust. *Rev. Geophys. Space Phys.*, 13:57–86.
- Crane, K., 1985. The spacing of rift axis highs: dependence upon diapiric processes in the underlying asthenosphere. *Earth Planet. Sci. Lett.*, 72:405–414.
- Daines, M.J., and Kohlstedt, D.L., 1997. Influence of deformation on melt topology in peridotites. *J. Geophys. Res.*, 102:10257–10271.
- Dick, H.J.B., 1989. Abyssal peridotites, very slow spreading ridges and ocean ridge magmatism. In Saunders, A.D., and Norry, M.J. (Eds.), *Magmatism in the Ocean Basins*. Spec. Publ.—Geol. Soc. London, 42:71–105.
- Dick, H.J.B., and Kelemen, P.B., 1992. Light rare earth element enriched clinopyroxene in harzburgites from 15°05'N on the Mid-Atlantic Ridge. *Eos*, 73:584.
- Dosso, L., Hanan, B.B., Bougault, H., Schilling, J.G., and Joron, J.L., 1991. Sr-Nd-Pb geochemical morphology between 10 degrees N and 17 degrees N on the Mid-Atlantic Ridge—a new MORB isotope signature. *Earth Planet. Sci. Lett.*, 106:29–43.
- Dunn, R.A., and Toomey, D.R., 1997. Seismological evidence for three-dimensional melt migration beneath the East Pacific Rise. *Nature*, 388:259–262.
- Elthon, D., Stewart, M., and Ross, D.K., 1992. Compositional trends of minerals in oceanic cumulates. *J. Geophys. Res.*, 97:15189–15199.

- Forsyth, D.W., Webb, S.C., Dorman, L.M., and Shen, Y., 1998. Phase velocities of Rayleigh waves in the MELT Experiment from the East Pacific Rise. *Science*, 280:1235–1237.
- Fujiwara, T., Lin, J., Matsumoto, T., Kelemen, P.B., Tucholke, B.E., and Casey, J.F., in press. Crustal Evolution of the Mid-Atlantic Ridge near the Fifteen-Twenty Fracture Zone in the last 5 Ma. *Geochem., Geophys., Geosys.*
- Ghose, I., Cannat, M., and Seyler, M., 1996. Transform fault effect on mantle melting in the MARK area (Mid-Atlantic Ridge south of the Kane transform). *Geology*, 24:1139–1142.
- Gillis, K., Mével, C., Allan, J., et al., 1993. *Proc. ODP, Init. Repts.*, 147: College Station, TX (Ocean Drilling Program).
- Hart, S.R., Schilling, J.-G., and Powell, J.L., 1973. Basalts from Iceland and along the Reykjanes Ridge: Sr isotope geochemistry. *Nature*, 246:104–107.
- Hurst, S.D., Gee, J.S., and Lawrence, R.M., 1997. Data report: Reorientation of structural features at Sites 920 to 924 using remanent magnetization and magnetic characteristics. In Karson, J.A., Cannat, M., Miller, D.J., and Elthon, D. (Eds.), *Proc. ODP, Sci. Results*, 153: College Station, TX (Ocean Drilling Program), 547–559.
- Ishizuka, H., Fujimoto, H., Bryan, W., Fujiwara, T., Furuta, T., Kelemen, P., Kinoshita, H., Kobayashi, K., Matsumoto, T., Takeuchi, A., and Tivey, M., 1995. Oceanic lower crust and upper mantle materials in transform fault zone of WMARK (Japanese with English abstr.). *JAMSTEC J. Deep Sea Res.*, 11:37–52.
- Jha, K., Parmentier, E.M., and Phipps Morgan, J., 1994. The role of mantle-depletion and melt-retention buoyancy in spreading-center segmentation. *Earth Planet. Sci. Lett.*, 125:221–234.
- Jousselin, D., Nicolas, A., and Boudier, F., 1998. Detailed mapping of a mantle diapir below a paleo-spreading center in the Oman ophiolite. *J. Geophys. Res.*, 103:18153–18170.
- Kelemen, P.B., Braun, M.G., Hirth, G., and Garrido, C.J., 1998a. Size/frequency statistics for dunite veins in the shallow mantle. *Eos*, 79:S225.
- Kelemen, P.B., Hirth, G., Shimizu, N., Spiegelman, M., and Dick, H.J.B., 1997. A review of melt migration processes in the asthenospheric mantle beneath oceanic spreading centers, *Phil. Trans. Roy. Soc. London*, A355:283–318.
- Kelemen, P.B., Matsumoto, T., and Shipboard Scientific Party, 1998b. Geological Results of MODE 98, Leg 1: JAMSTEC/WHOI Shinkai 6500 Cruise to 15 N, Mid-Atlantic Ridge. *Eos*, 79:F45.
- Kelemen, P.B., Shimizu, N., and Salters, V.J.M., 1995a. Extraction of mid-ocean-ridge basalt from the upwelling mantle by focused flow of melt in dunite channels. *Nature*, 375:747–753.
- Kelemen, P.B., Whitehead, J.A., Aharonov, E., and Jordahl, K.A., 1995b. Experiments on flow focusing in soluble porous media, with applications to melt extraction from the mantle. *J. Geophys. Res.*, 100:475–496.
- Kelso, P.R., Richter, C., and Pariso, J.E., 1996. Rock magnetic properties, magnetic mineralogy, and paleomagnetism of peridotites from Site 895, Hess Deep. In Mével, C., Gillis, K.M., Allan, J.F., and Meyer, P.S. (Eds.), *Proc. ODP, Sci. Results*, 147: College Station, TX (Ocean Drilling Program), 405–413.

- Kikawa, E., Kelso, P.R., Pariso, J.E., and Richter, C., 1996. Paleomagnetism of gabbroic rocks and peridotites from Sites 894 and 895, Leg 147, Hess Deep: results of half-core and whole-core measurements. *In* Mével, C., Gillis, K.M., Allan, J.F., and Meyer, P.S. (Eds.), *Proc. ODP, Sci. Results*, 147: College Station, TX (Ocean Drilling Program), 383–391.
- Kohlstedt, D.L., and Zimmerman, M.E., 1996. Rheology of partially molten mantle rocks. *Ann. Rev. Earth Planet. Sci.*, 24:41–62.
- Kuo, B.-Y., and Forsyth, D.W., 1988. Gravity anomalies of the ridge transform system in the South Atlantic between 31° and 34°S. *Mar. Geophys. Res.*, 10:205–232.
- Langmuir, C.H., and Bender, J.F., 1984. The geochemistry of oceanic basalts in the vicinity of transform faults: observations and implications. *Earth Planet. Sci. Lett.*, 69:107–127.
- Lawrence, R.M., Gee, J.S., and Hurst, S.D., 1997. Magnetic anisotropy in serpentinized peridotites from Site 920: its origin and relationship to deformation fabrics. *In* Karson, J.A., Cannat, M., Miller, D.J., and Elthon, D. (Eds.), *Proc. ODP, Sci. Results*, 153: College Station, TX (Ocean Drilling Program), 419–427.
- Lin, J., and Phipps Morgan, J., 1992. The spreading rate dependence of three-dimensional midocean ridge gravity structure. *Geophys. Res. Lett.*, 19:13–16.
- Lin, J., Purdy, G.M., Schouten, H., Sempéré, J.-C., and Zervas, C., 1990. Evidence from gravity data for focused magmatic accretion along the Mid-Atlantic Ridge. *Nature*, 344:627–632.
- Magde, L.S., Dick, H.J.B., and Hart, S.R., 1995. Tectonics, alteration and the fractal distribution of hydrothermal veins in the lower ocean crust. *Earth Planet. Sci. Lett.*, 129:103–119.
- Magde, L.S., Sparks, D.W., and Detrick, R.S., 1997. The relationship between buoyant mantle flow, melt migration, and gravity bull's eyes at the Mid-Atlantic Ridge between 33°N and 35°N. *Earth Planet. Sci. Lett.*, 148:59–67.
- Matsumoto, T., Kelemen, P.B., and O.S. Party, 1998. Preliminary results of the precise geological and geophysical mapping of the Mid-Atlantic Ridge 14–16 N—tectonic extension along the magma-poor ridge axis. *Eos*, 79:F46.
- Miller, D.J., and Christensen, N.I., 1997. Seismic velocities of lower crustal and upper mantle rocks from the slow-spreading Mid-Atlantic Ridge, south of the Kane Transform Zone (MARK). *In* Karson, J.A., Cannat, M., Miller, D.J., and Elthon, D. (Eds.), *Proc. ODP, Sci. Results*, 153: College Station, TX (Ocean Drilling Program), 437–454.
- Nicolas, A., 1986. A melt extraction model based on structural studies in mantle peridotites. *J. Petrol.*, 27:999–1022.
- , 1990. Melt extraction from mantle peridotites: hydrofracturing and porous flow, with consequences for oceanic ridge activity. *In* Ryan, M.P. (Ed.), *Magma Transport and Storage*: Chichester (Wiley), 159–173.
- Nicolas, A., and Boudier, F., 1995. Mapping oceanic ridge segments in Oman ophiolites. *J. Geophys. Res.*, 100:6179–6197.
- Nicolas, A., Boudier, F., and Ildefonse, B., 1996. Variable crustal thickness in the Oman ophiolite: implication for oceanic crust. *J. Geophys. Res.*, 101:17941–17950.
- Nicolas, A., and Rabinowicz, M., 1984. Mantle flow pattern at oceanic spreading centres: relation with ophiolitic and oceanic structures. *In* Gass, I.G., Lippard, S.J., and

- Shelton, A.W., (Eds.), *Ophiolites and Oceanic Lithosphere*, Spec. Publ.—Geol. Soc. London, 13:147–151.
- Nicolas, A., and Violette, J.F., 1982. Mantle flow at oceanic spreading centers: models derived from ophiolites. *Tectonophysics*, 81:319–339.
- Parmentier, E.M., and Phipps Morgan, J., 1990. Spreading rate dependence of three-dimensional structure in oceanic spreading centers. *Nature*, 348:325–328.
- Peyve, A.A., Raznitsin, Y.N., Lyapunov, S.M., and Scolotnev, S.G., 1988a. Mantle heterogeneity in the area of Cape Verde Fracture Zone in the central Atlantic according to the data on basalts (in Russian). *Dok. Acad. Sci. USSR*, 301:165–168.
- Peyve, A.A., Suchevskaya, N.M., Lyapunov, S.M., and Konokova, N.N., 1988b. Peculiarities of tholeiitic magmatism in the area of the Cape Verde Fracture Zone in the Atlantic (13°–15°N) (in Russian). *Dok. Acad. Sci. USSR*, 302:1174–1178.
- Phipps Morgan, J., 1987. Melt migration beneath mid-ocean spreading centers, *Geophys. Res. Lett.*, 14:1238–1241.
- Phipps Morgan, J., and Forsyth, D.W., 1988. Three-dimensional flow and temperature perturbations due to a transform offset: effects on oceanic crustal and upper mantle structure, *J. Geophys. Res.*, 93:2955–2966.
- Rabinowicz, M., Ceuleneer, M., and Nicolas, A., 1987. Melt segregation and flow in mantle diapirs below spreading centers: evidence from the Oman ophiolites. *J. Geophys. Res.*, 92:3475–3486.
- Rabinowicz, M., Nicolas, A., and Vigneresse, J.L., 1984. A rolling mill effect in asthenosphere beneath oceanic spreading centers. *Earth Planet. Sci. Lett.*, 67:97–108.
- Richter, C., Kelso, P.R., and MacLeod, C.J., 1996. Magnetic fabrics and sources of magnetic susceptibility in lower crustal and upper mantle rocks from Hess Deep. In Mével, C., Gillis, K.M., Allan, J.F., and Meyer, P.S. (Eds.), *Proc. ODP, Sci. Results*, 147: College Station, TX (Ocean Drilling Program), 393–403.
- Schilling, J.-G., 1973. Iceland mantle plume: geochemical study of Reykjanes Ridge. *Nature*, 242:565–571.
- Schouten, H., Klitgord, K.D., and Whitehead, J.A., 1985. Segmentation of mid-ocean ridges. *Nature*, 317:225–229.
- Seyler, M., and Bonatti, E., 1997. Regional-scale melt-rock interaction in lherzolitic mantle in the Romanche Fracture Zone (Atlantic Ocean), *Earth Planet. Sci. Lett.*, 146:273–287.
- Silant'ev, S.A., Dmitriev, L.V., Bazylev, B.A., Casey, J.F., Bougault, H., Levsky, L.K., Belyatsky, B.V., and Ovchinnikova, G.V., 1996. An examination of genetic conformity between co-existing basalt, gabbro and residual peridotites from 15°20'N fracture zone, central Atlantic: evidence from isotope composition of Sr, Nd, and Pb, *InterRidge Newsletter*, 4:18–21.
- Sobolev, A.V., Dmitriev, L.V., Tsamerian, O.P., Simonov, V.A., Skolotnev, S.G., and Basilev, B.A., 1992a. On the structure and origin of geochemical anomaly in basalts from Mid-Atlantic Ridge between 12 and 18°N (in Russian). *Dok. Akad. Nauk USSR*, 326:541–546.

- Sobolev, A.V., Tsamerian, O.P., and Dmitriev, L.V., 1992b. The geochemical anomaly in Mid-Atlantic Ridge basalts between 12°–18°N: geochemical structure and origin. *Proc. 29th International Geol. Cong.*, 29:58.
- Sobolov, A.V., Tsamerian, G.P., Dmitriev, L.V., and Basilev, B., 1992. The correlation between the mineralogy of basalt and the associated peridotites: the data from the MAR between 8°–18°N. *Eos*, 73:584.
- Sparks, D.W., and Parmentier, E.M., 1991. Melt extraction from the mantle beneath spreading centers. *Earth Planet. Sci. Lett.*, 105:368–377.
- , 1993. The structure of three-dimensional convection beneath oceanic spreading centres. *Geophys. J. Int.*, 112:81–91.
- , 1994. The generation and migration of partial melt beneath oceanic spreading centers. In Ryan, M.P. (Ed), *Magmatic Systems*: San Diego CA, (Academic Press, Inc.), 55-76.
- Sparks, D.W., Parmentier, E.M., and Phipps Morgan, J., 1993. Three-dimensional mantle convection beneath a segmented spreading center; implications for along-axis variations in crustal thickness and gravity. *J. Geophys. Res.*, 98:21977–21995.
- Spiegelman, M., 1993. Physics of melt extraction: theory, implications and applications. *Phil. Trans. Roy. Soc. London A.*, 342:23–41.
- Spiegelman, M., and McKenzie, D., 1987. Simple 2-D models for melt extraction at mid-ocean ridges and island arcs. *Earth Planet. Sci. Lett.*, 83:137–152.
- Staudacher, T., Sarda, P., Richardson, S.H., Allegre, C.J., Sagna, I., and Dimitriev, L.V., 1989. Noble gases in basalt glasses from a Mid-Atlantic Ridge topographic high at 14°N: geodynamic consequences. *Earth Planet. Sci. Lett.*, 96:119–133.
- Su, W., and Buck, W.R., 1993. Buoyancy effects on mantle flow under mid-ocean ridges. *J. Geophys. Res.*, 98:12191–12205.
- Team, T.M.S., 1998. Imaging the deep seismic structure beneath a mid-ocean ridge: the MELT experiment. *Science*, 280:1215–1218.
- Tolstoy, M.A., Harding, J.A., and Orcutt, J.A., 1992. Crustal thickness at the Mid-Atlantic Ridge: bull's eye gravity anomalies and focused accretion. *Science*, 262:726–729.
- Toomey, D.R., Wilcock, W.S.D., Solomon, S.C., Hammond, W.C., and Orcutt, J.A., 1998. Mantle seismic structure beneath the MELT region of the East Pacific Rise from P and S wave tomography. *Science*, 280:1224–1227.
- Tucholke, B.E., Lin, J., Kleinrock, M.C, Tivey, M.A., Reed, T.B., Goff, J., and Jaroslow, G., 1997. Segmentation and crustal structure of the western Mid-Atlantic Ridge flank, 25°25'–27°10'N and 0–29 m.y. *J. Geophys. Res.*, 102:10203–10223.
- Turcotte, D.L., and Phipps Morgan, J., 1992. The physics of melt migration and mantle flow beneath a mid-ocean ridge. In Phipps Morgan, J., Blackman D., and Sinton, J. (Eds.), *Mantle Flow and Melt Generation at Mid-Ocean Ridges*. Geophys. Mono., 71:155–182.
- White, R.S., McKenzie, D., and O'Nions, R.K., 1992. Oceanic crustal thickness from seismic measurements and rare earth element inversions. *J. Geophys. Res.*, 97:19683–19715.
- Whitehead, J.A., Dick, H.J.B., and Shouten, H., 1984. A mechanism for magmatic accretion under spreading centers. *Nature*, 312:146–148.

Xia, C., Casey, J.F., Silantiev, S., and Dmitriev, L., 1991. Geochemical structure of the 14°N mantle source anomaly along the Mid-Atlantic Ridge and geochemical changes across the 15°20'N Fracture Zone. *Eos*, 72:518.

Xia, C., Casey, J.F., Silantiev, S., Dmitriev, L., and Bougault, H., 1992. Geochemical variations between 12° to 16°N, Mid-Atlantic Ridge: a region with high degrees of partial melting yet magma starved? *Eos*, 73:553.

TABLE CAPTIONS

Table T1. Operations plan and time estimate for primary sites, ODP Leg 209.

Table T2. Time estimates for Leg 209 wireline logging.

Table T3. Site survey data.

FIGURE CAPTIONS

- Figure F1.** Preliminary calculation of Mantle Bouger Anomaly (e.g., Lin et al., 1990) from shipboard gravity measurements in 1998 (Kelemen et al., 1998b; Matsumoto et al., 1998; Casey et al., 1998). Both figures use the same range of colors, representing slightly different values. **A.** Range is from about -35 (red) to $+40$ (pink) Mgal north of the $15^{\circ}20'N$ FZ. **B.** Range is from about -60 (red) to $+45$ (pink) Mgal south of the $15^{\circ}20'N$ FZ. These data suggest that the magma-starved region with abundant peridotite outcrops from $14^{\circ}40'$ to $15^{\circ}40'N$ lies on the periphery of large magmatic segments centered at $\sim 14^{\circ}$ and $16^{\circ}N$, with thick igneous crust in the segment centers.
- Figure F2.** Bathymetry and geology from 14° to $16^{\circ}N$ along the Mid-Atlantic Ridge. Depth range is ~ 5400 (violet) to 1600 (red) m. Sample lithologies are compiled from all known dredging and submersible results. **A.** North of $15^{\circ}20'N$ FZ. **B.** South of $15^{\circ}20'N$ FZ. **C.** View from the north of the “megamullion” dive site, where a large low-angle normal fault is exposed on the seafloor. Open circles = mantle peridotite, solid circles = basalt.
- Figure F3.** Geochemical data on samples from the Mid-Atlantic Ridge. **A.** Low Na_2O (upper panel data from the equator to $70^{\circ}N$, lower panel data from 10° to $20^{\circ}N$) in basalts. **B.** High $Cr/(Cr+Al)$ in spinel (lower panel) and shallow axial depth (upper panel) can all be taken to indicate high degrees of partial melting. **C.** High La/Sm (upper panel data from the equator to $70^{\circ}N$, lower panel data from 10° to $20^{\circ}N$). **D.** High $^{206}Pb/^{204}Pb$ (upper panel) and high $^{87}Sr/^{86}Sr$ (lower panel). **C** and **D** are indicative of long-term enrichment of the mantle source in incompatible trace elements. All of these characteristics are observed along the Mid-Atlantic Ridge just south of the $15^{\circ}20'N$ Fracture Zone (FZ). Basalt data compiled by Xia et al. (1991, 1992) and Casey et al. (1992). Spinel data and bathymetry from Bonatti et al. (1992) and Sobolev et al. (1991, 1992a).
- Figure F4.** **A.** Maps showing locations of conventional seismic refraction profiles (long white lines) and NOBEL experiments (numbered black lines) in 1997. **B–D.** Preliminary interpretation of data from the long refraction profile (R. Detrick and J. Collins, pers. comm., 1998); **(B)** 2-D velocity model with contours labeled in kilometers per second, **(C)** indication of data coverage, which is sparse in the lower crust but sufficient to define large, lateral velocity variations (contours labeled in kilometers per second), and **(D)** traveltimes data (circles) with model calculations (shading) for comparison. **E.** Comparison of two one-dimensional sections through the velocity model with a typical one-dimensional section for oceanic crust at the East Pacific Rise (EPR). MAR = Mid-Atlantic Ridge.
- Figure F5.** Proposed drill sites, including alternates. Please see Table T3 and site data sheets for submersible dives and lithologies associated with each site.
- Figure F6.** **A.** Schematic diagram drawn after Barnouin-Jha et al. (1997) showing results for the upper 50 km in a dynamic model of buoyancy-driven 3-D mantle flow beneath a slow-spreading ridge. Red = flow vectors in the horizontal plane, yellow = flow vectors in the vertical ridge-axis plane, blue = flow vectors in the vertical ridge-normal plane. This illustrates along-axis flow in the shallow mantle from

segment centers to segment ends. Note spacing between upwelling centers is ~400 km and the region of melt generation is almost as long as the ridge segments. **B.** From Ceuleneer (1991), illustrating ductile flow vectors and shear sense inferred from peridotite fabrics in the mantle section of the Maqsad area, Oman ophiolite. Map area is ~17 km long × 14 km wide. Approximate location of inferred paleoridge axis is shown as a red line. **C.** Schematic diagram from Joussetin et al. (1998) showing their vision of mantle flow, based on observations from the Oman ophiolite, with a narrow zone of upwelling and a thin region of corner flow feeding a ridge segment that is three times longer than the diameter of the mantle upwelling zone. This model requires extensive subhorizontal ridge-parallel flow of residual mantle peridotite from the segment center to the segment ends. Although this geometry seems somewhat extreme and has not been produced in any 3-D dynamic model to date, it illustrates the type of highly focused solid upwelling that could produce the observed along-axis variation in crustal thickness on the Mid-Atlantic Ridge via 3-D focusing of mantle flow. Dynamic models such as that illustrated in A do not have sufficiently narrow zones of mantle upwelling and cannot reproduce the lengths of observed magmatic segments (~30–100 km). MOHO = Mohorovicic seismic discontinuity.

Table T1. Operations plan and time estimate for primary sites, ODP Leg 209.

Site	Location (lat/long)	Water depth (mbrf)	Operations description	(hrs)	Total transit (days)	Total coring (days)	Total logging (days)	Total on-site (days)
22.53°S, 43.17°W Begin leg in Rio de Janeiro, Brazil				120.0				
Transit ~2246 nmi from Rio de Janeiro to MAR-4S @ 10.5 kt				214.0	8.9			
MAR-4S	14.8488°N	3011	Hole A: Bare rock spud/RCB core minimum 100+ mbsf half cores)	134.0		5.6		
	45.0822°W		(wireline logging with triple combo and FMS-sonic)	14.0			0.6	6.2
Transit ~5 nmi from MAR-4S to MAR-3S @ 10.5 kt				2.0	0.1			
MAR-3S	14.9324°N	2861	Hole A: Bare rock spud/RCB core minimum 100+ mbsf half cores)	118.0		4.9		
	45.0713°W		(wireline logging with triple combo and FMS-sonic)	14.0			0.6	5.5
Transit ~53 nmi from MAR-3S to MAR-1S @ 10.5 kt				5.0	0.2			
MAR-1S	15.1090°N	2911	Hole A: Bare rock spud/RCB core minimum 100+ mbsf half cores)	118.0		4.9		
	44.9590°W		(wireline logging with triple combo and FMS-sonic)	14.0			0.6	5.5
Transit ~105 nmi from MAR-1S to MAR-1N @ 10.5 kt				10.0	0.4			
MAR-1N	15.6478°N	3981	Hole A: Bare rock spud/RCB core minimum 100+ mbsf half cores)	130.0		5.4		
	46.6759°W		(wireline logging with triple combo and FMS-sonic)	15.0			0.6	6.0
Transit ~6 nmi from MAR-1N to MAR-2N @ 10.5 kt				2.0	0.1			
MAR-2N	15.5480°N	3911	Hole A: Bare rock spud/RCB core minimum 100+ mbsf half cores)	127.0		5.3		
	46.6870°W		(wireline logging with triple combo and FMS-sonic)	15.0			0.6	5.9
Transit ~3 nmi from MAR-2N to MAR-3N @ 10.5 kt				2.0	0.1			
MAR-3N	15.5000°N	3451	Hole A: Bare rock spud/RCB core minimum 100+ mbsf half cores)	123.0		5.1		
	46.6810°W		(wireline logging with triple combo and FMS-sonic)	14.0			0.6	5.7
Transit ~104 nmi from MAR-3N to MAR-2S @ 10.5 kt				10.0	0.4			
MAR-2S	15.0390°N	3611	Hole A: Bare rock spud/RCB core minimum 100+ mbsf half cores)	132.0		5.5		
	44.9530°W		(wireline logging with triple combo and FMS-sonic)	15.0			0.6	6.1
Transit ~1482 nmi from MAR-2S to Bermuda @ 10.5 kt				142.0	5.9			
32.18°N, 64.48°W End leg in Hamilton, Bermuda								
SUBTOTAL:					16.1	36.8	4.2	41.0
TOTAL OPERATING HOURS/DAYS (incl. 5.0 day port call):					1490.0		62.1	

- Note 1: multiple spud attempts may be required at each site in order to advance a single RCB hole to minimum of 100 mbsf.
- Note 2: penetration depths beyond 100 mbsf are desired and will be pursued if hole conditions allow.
- Note 3: wireline logging may be problematic at all or some of the drilling locations. As a result, RAB-C logging-while-coring (LWC) will likely be substituted for conventional RCB coring and/or wireline logging at selected sites.
- Note 4: desired coring approach is to cut/recover RCB half cores using non-magnetic core barrels with chrome plated ID.

Table T2. Time estimates for Leg 209 wireline logging.

Site	Tool strings	Hole depth* (mbsf)	Time (hr)
MAR-4S	Triple combo and FMS/sonic	100	14.0
MAR-3S	Triple combo and FMS/sonic	100	13.8
MAR-1S	Triple combo and FMS/sonic	100	13.9
MAR-1N	Triple combo and FMS/sonic	100	15.3
MAR-2N	Triple combo and FMS/sonic	100	15.2
MAR-3N	Triple combo and FMS/sonic	100	14.6
MAR-2S	Triple combo and FMS/sonic	100	14.8

Note: * = hole depths are estimated based on potential bit life for a single hole penetration.

Table T3. Site survey data.

Site	Latitude	Longitude	Water depth (mbsl)	Survey dive number	Bedrock
Primary sites					
MAR-1N	15.6478°N	46.6759°W	3970	MODE 98, Leg 1, dive 416	Peridotite
MAR-2N	15.5480°N	46.6870°W	3900	Faranaut 92, dive 20	Peridotite
MAR-3N	15.5000°N	46.6810°W	3440	Faranaut 92, dive 16	Peridotite
MAR-1S	15.1090°N	44.9590°W	2900	Faranaut 92, dive 5	Peridotite
MAR-2S	15.0390°N	44.9530°W	3600	Faranaut 92, dive 7	Peridotite
MAR-3S	14.9324°N	45.0713°W	2850	MODE 98, Leg 1, dive 423	Gabbro and peridotite
MAR-4S	14.8488°N	45.0822°W	3000	MODE 98, Leg 1, dive 427	Peridotite
Alternate sites					
MAR-Alt-1N	15.7358°N	46.9022°W	1680	MODE 98, Leg 1, dive 422	Gabbro and peridotite
MAR-Alt-2N	15.6130°N	46.5760°W	3600	Faranaut 92, dive 10	Peridotite
MAR-Alt-1S	15.1167°N	45.2667°W	1650	No dive survey	Probably peridotite
MAR-Alt-2S	14.7226°N	44.8922°W	2075	MODE 98, Leg 1, dive 425	Peridotite

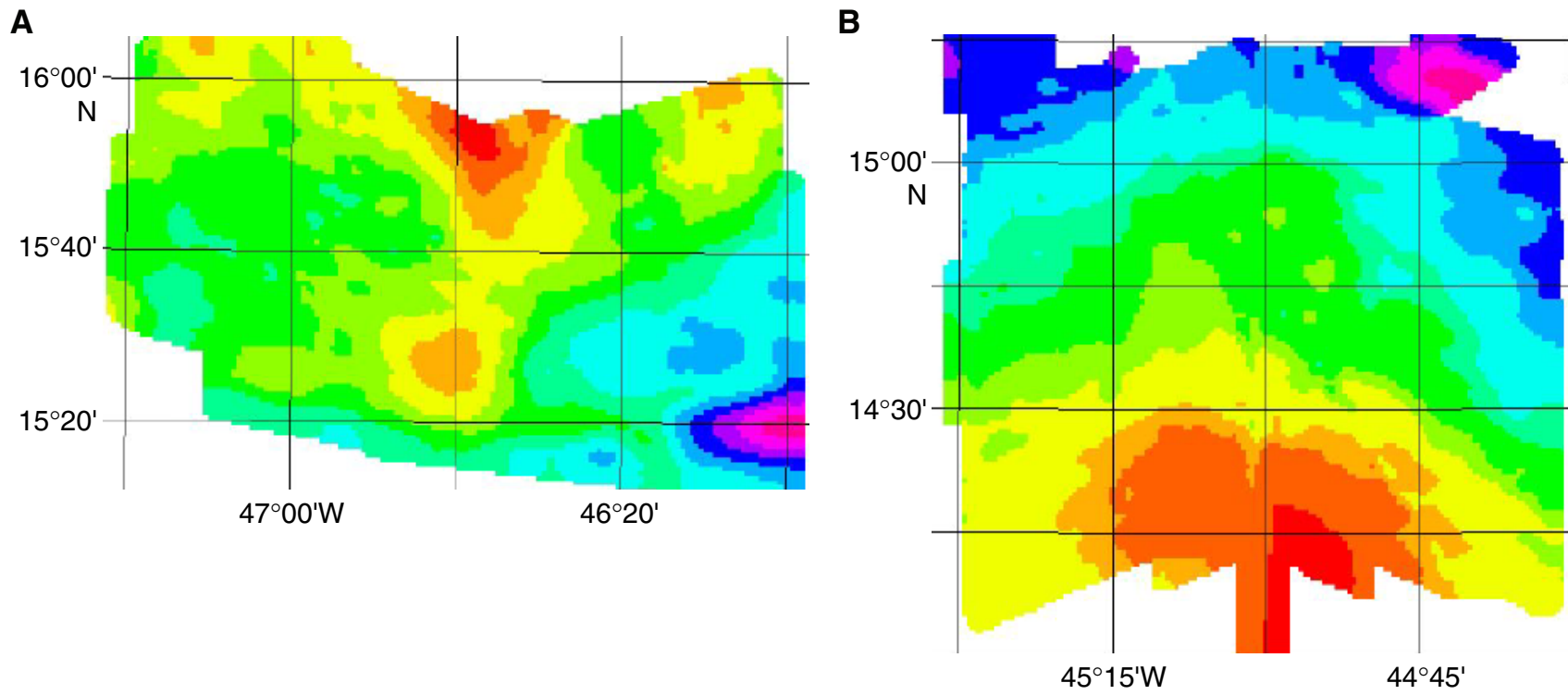


Figure F1

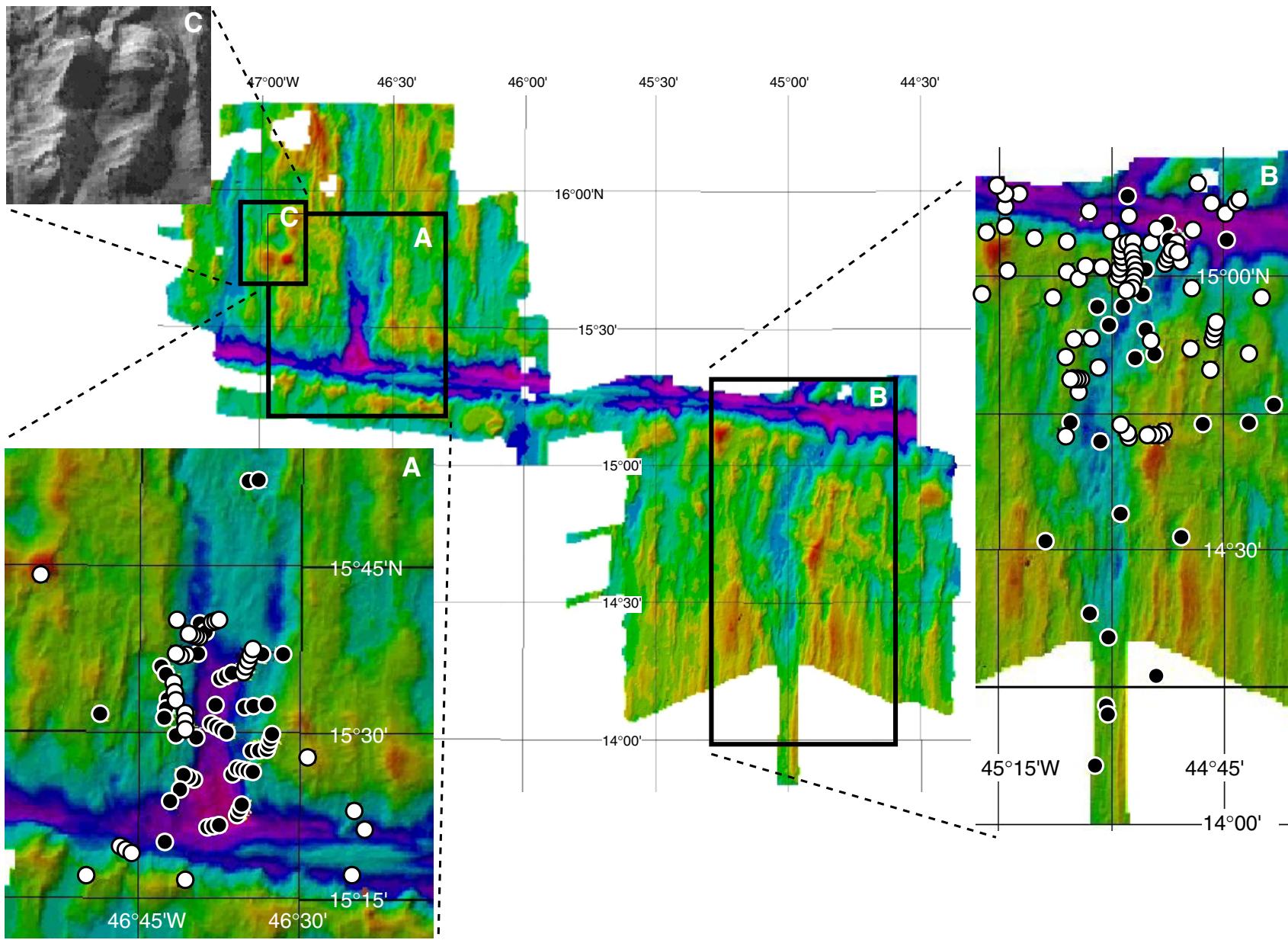


Figure F2

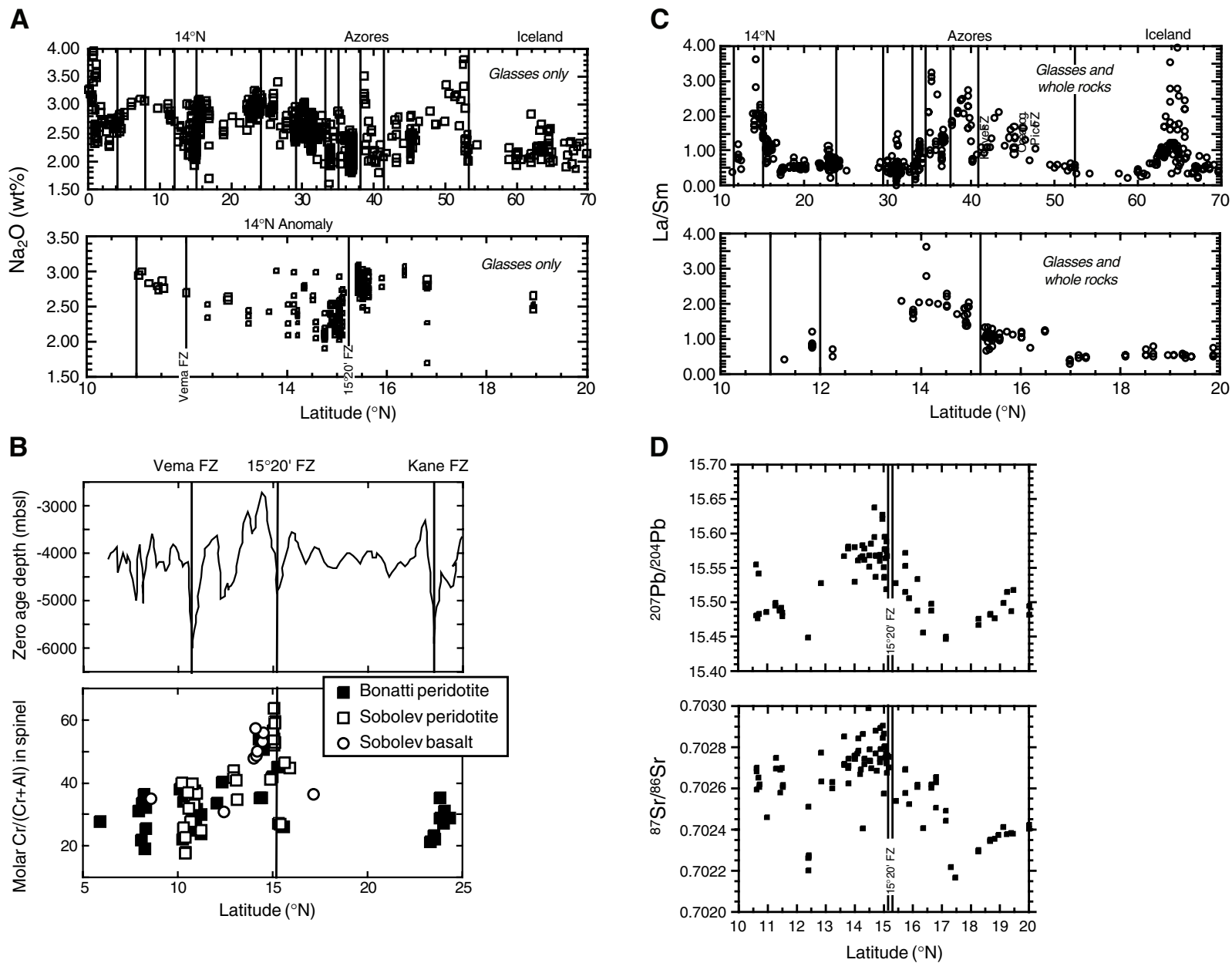


Figure F3

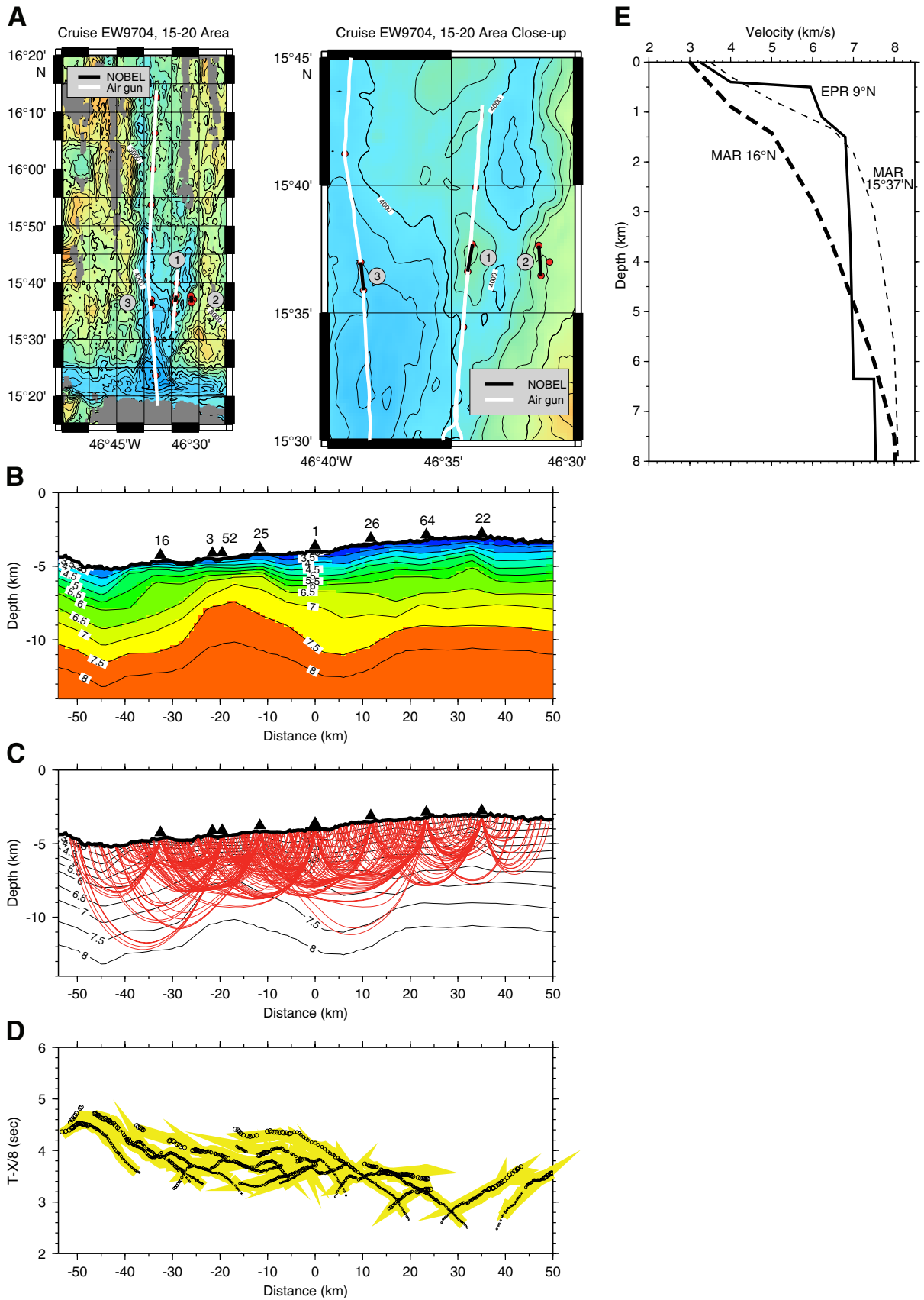


Figure F4

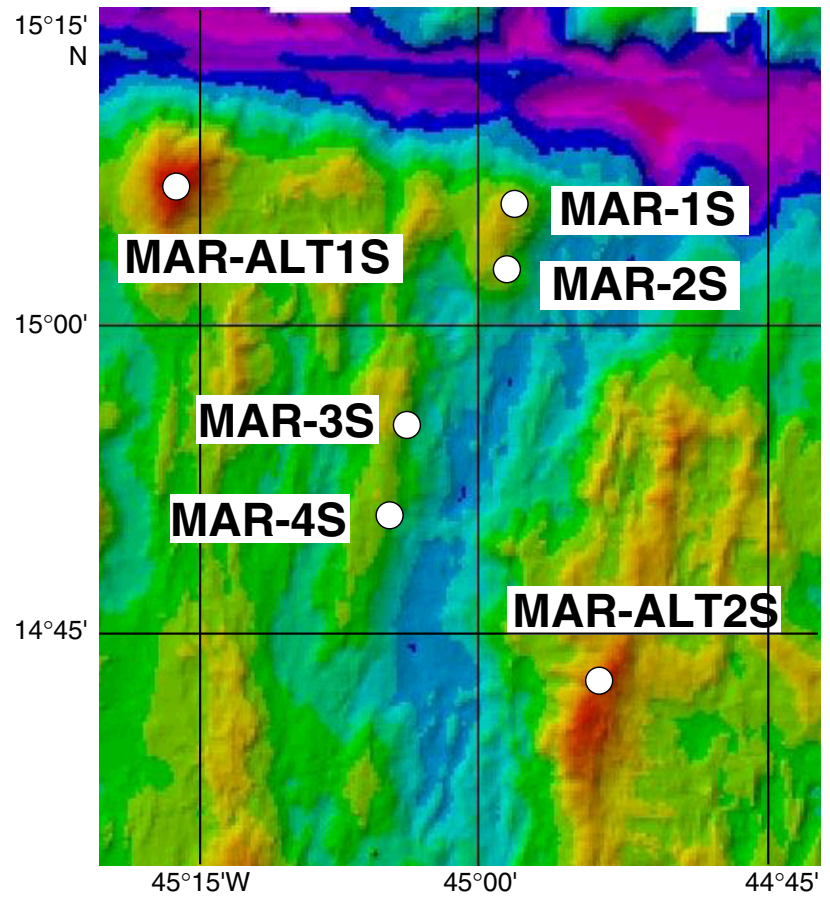
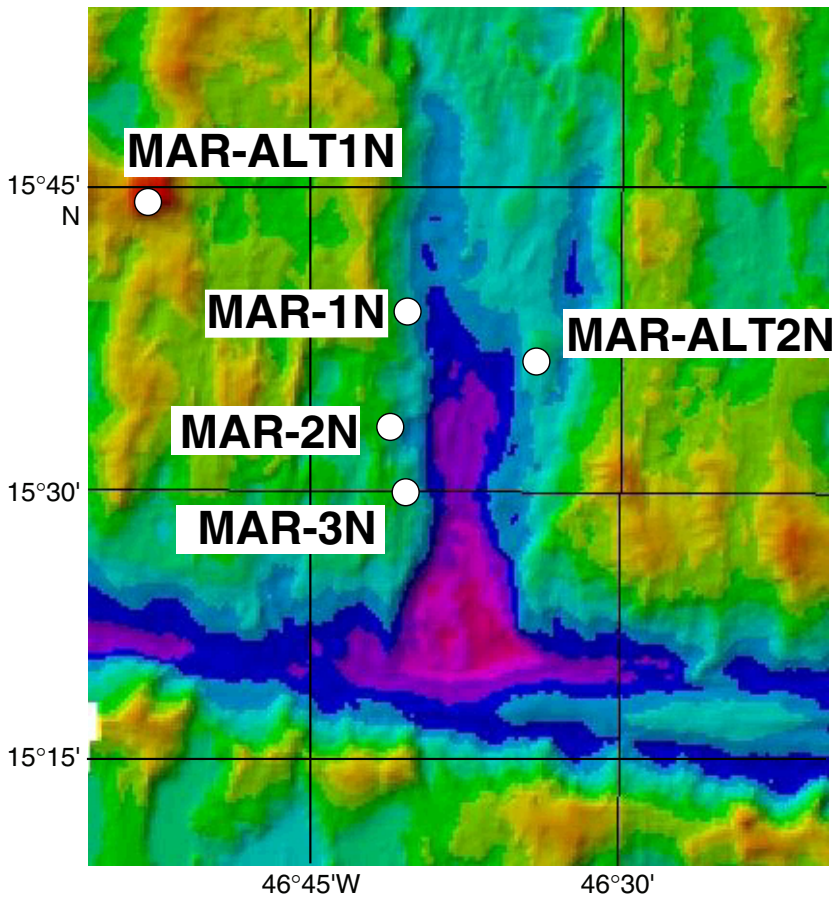


Figure F5

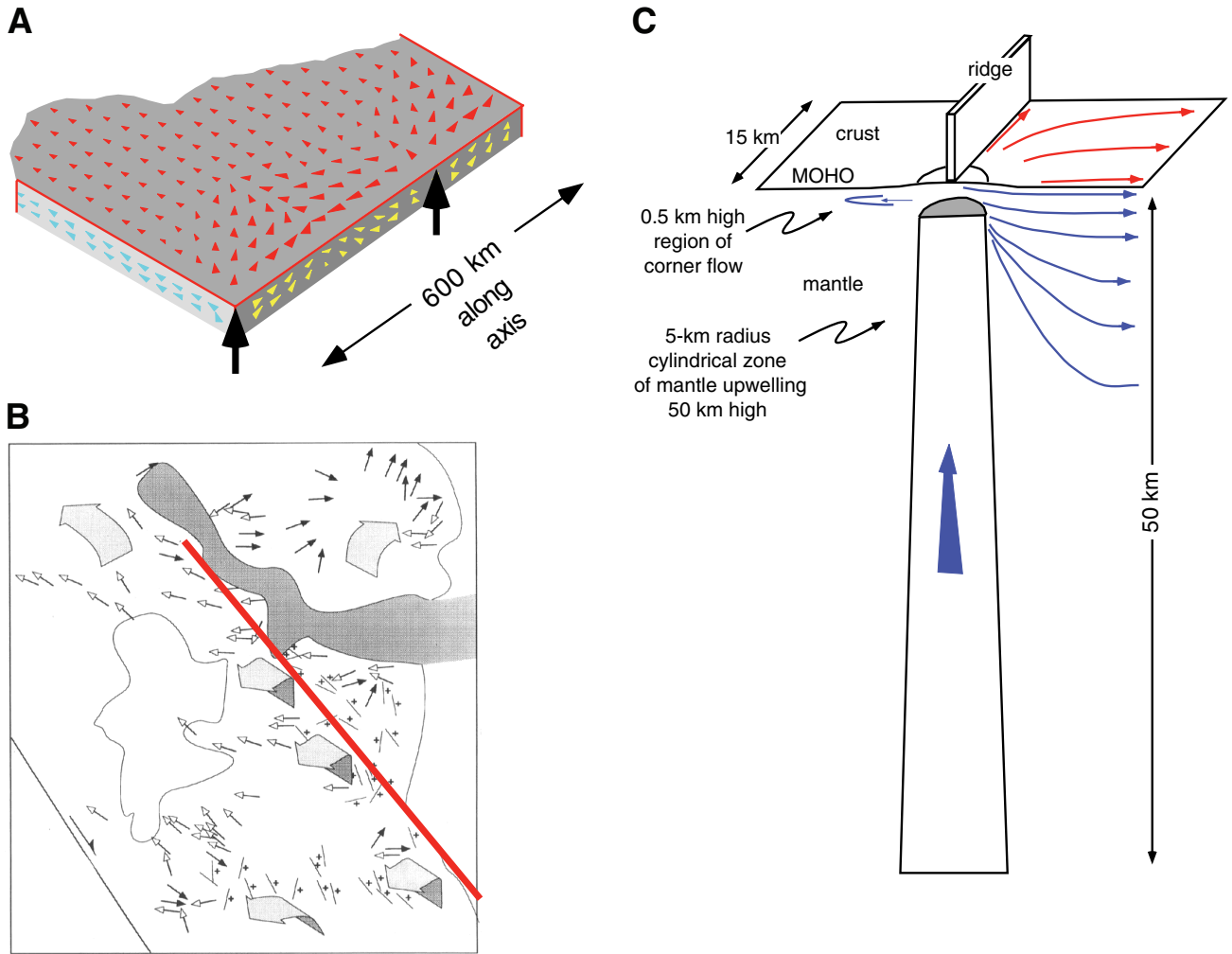


Figure F6

SITE SUMMARIES

Site: MAR-1N

Priority: Primary

Position: 15.6478°N, 46.6759°W

Water Depth: 3970 mbsl (3981 mbrf)

Target Drilling Depth: 300 mbsf

Approved Maximum Penetration: 300 mbsf

Survey Coverage: MODE 98, Leg 1, dive 416

Objective: Northernmost of a transect of three sites on the west wall of the Mid-Atlantic Ridge rift valley sampling serpentinized peridotite from near the ridge segment center north of the 15°20'N Fracture Zone to near the segment end.

Drilling Program: Single bit penetration as deep as possible or 300 mbsf.

Logging Program: Two logging runs, triple combo and FMS-sonic if hole conditions permit.

Nature of Rock Anticipated: Serpentinized peridotite.

Site: MAR-2N

Priority: Primary

Position: 15.5480°N, 46.6870°W

Water Depth: 3900 mbsl (3911 mbrf)

Target Drilling Depth: 300 mbsf

Approved Maximum Penetration: 300 mbsf

Survey Coverage: *Faranaut 92*, dive 20

Objective: Center site in a transect of three sites on the west wall of the Mid-Atlantic Ridge rift valley sampling serpentized peridotite from near the ridge segment center north of the 15°20'N Fracture Zone to near the segment end.

Drilling Program: Single bit penetration as deep as possible or 300 mbsf.

Logging Program: Two logging runs, triple combo and FMS-sonic if hole conditions permit.

Nature of Rock Anticipated: Serpentized peridotite.

Site: MAR-3N

Priority: Primary

Position: 15.5000°N, 46.6810°W

Water Depth: 3440 mbsl (3451 mbrf)

Target Drilling Depth: 300 mbsf

Approved Maximum Penetration: 300 mbsf

Survey Coverage: *Faranaut 92*, dive 16

Objective: Southernmost in a transect of three sites on the west wall of the Mid-Atlantic Ridge rift valley sampling serpentinized peridotite from near the ridge segment center north of the 15°20'N Fracture Zone to near the segment end.

Drilling Program: Single bit penetration as deep as possible or 300 mbsf.

Logging Program: Two logging runs, triple combo and FMS-sonic if hole conditions permit.

Nature of Rock Anticipated: Serpentinized peridotite.

Site: MAR-1S

Priority: Primary

Position: 15.1090°N, 44.9590°W

Water Depth: 2900 mbsl (2911 mbrf)

Target Drilling Depth: 300 mbsf

Approved Maximum Penetration: 300 mbsf

Survey Coverage: *Faranaut 92*, dive 5

Objective: Northernmost in a transect of four sites on the west wall of the Mid-Atlantic Ridge (MAR) rift valley sampling serpentized peridotite from the inside corner high south of the intersection of the MAR and the 15°20'N Fracture Zone toward the center of the segment.

Drilling Program: Single bit penetration as deep as possible or 300 mbsf.

Logging Program: Two logging runs, triple combo and FMS-sonic if hole conditions permit.

Nature of Rock Anticipated: Serpentized peridotite.

Site: MAR-2S

Priority: Primary

Position: 15.0390°N, 44.9530°W

Water Depth: 3600 mbsl (3611 mbrf)

Target Drilling Depth: 300 mbsf

Approved Maximum Penetration: 300 mbsf

Survey Coverage: *Faranaut 92*, dive 7

Objective: Intermediate site in a transect of four sites on the west wall of the Mid-Atlantic Ridge (MAR) rift valley sampling serpentized peridotite from the inside corner high south of the intersection of the MAR and the 15°20'N Fracture Zone toward the center of the segment.

Drilling Program: Single bit penetration as deep as possible or 300 mbsf.

Logging Program: Two logging runs, triple combo and FMS-sonic if hole conditions permit.

Nature of Rock Anticipated: Serpentized peridotite.

Site: MAR-3S

Priority: Primary

Position: 14.9324°N, 45.0713°W

Water Depth: 2850 mbsl (2861 mbrf)

Target Drilling Depth: 300 mbsf

Approved Maximum Penetration: 300 mbsf

Survey Coverage: MODE 98, Leg 1, dive 423

Objective: Intermediate site in a transect of four sites on the west wall of the Mid-Atlantic Ridge (MAR) rift valley sampling serpentized peridotite from the inside corner high south of the intersection of the MAR and the 15°20'N Fracture Zone toward the center of the segment.

Drilling Program: Single bit penetration as deep as possible or 300 mbsf.

Logging Program: Two logging runs, triple combo and FMS-sonic if hole conditions permit.

Nature of Rock Anticipated: Serpentized peridotite.

Site: MAR-4S

Priority: Primary

Position: 14.8488°N, 45.0822°W

Water Depth: 3000 mbsl (3011 mbrf)

Target Drilling Depth: 300 mbsf

Approved Maximum Penetration: 300 mbsf

Survey Coverage: MODE 98, Leg 1, dive 427

Objective: Intermediate site in a transect of four sites on the west wall of the Mid-Atlantic Ridge (MAR) rift valley sampling serpentized peridotite from the inside corner high south of the intersection of the MAR and the 15°20'N Fracture Zone toward the center of the segment.

Drilling Program: Single bit penetration as deep as possible or 300 mbsf.

Logging Program: Two logging runs, triple combo and FMS-sonic if hole conditions permit.

Nature of Rock Anticipated: Serpentized peridotite.

Site: MAR-ALT1N

Priority: Alternate

Position: 15.7358°N, 46.9022°W

Water Depth: 1680 mbsl (1691 mbrf)

Target Drilling Depth: 300 mbsf

Approved Maximum Penetration: 300 mbsf

Survey Coverage: MODE 98, Leg 1, dive 422

Objective: Located on the summit of a “megamullion” structure, interpreted as a low-angle normal fault surface exposed on the seafloor for ~100 km². Farthest north site in the region from which peridotite samples have been recovered.

Drilling Program: Single bit penetration as deep as possible or 300 mbsf.

Logging Program: Two logging runs, triple combo and FMS-sonic if hole conditions permit.

Nature of Rock Anticipated: Serpentinized peridotite.

Site: MAR-ALT2N

Priority: Alternate

Position: 15.6130°N, 46.5760°W

Water Depth: 3600 mbsl (3611 mbrf)

Target Drilling Depth: 300 mbsf

Approved Maximum Penetration: 300 mbsf

Survey Coverage: *Faranaut 92*, dive 10

Objective: Located on a small topographic dome within a broad part of the axial valley. Also the site of one of the NOBEL seismic experiments in 1997. If it is determined on the basis of the NOBEL results to be a place where unaltered or only slightly serpentinitized peridotite is <200 mbsf, then it could become a high-priority drilling target.

Drilling Program: Single bit penetration as deep as possible or 300 mbsf.

Logging Program: Two logging runs, triple combo and FMS-sonic if hole conditions permit.

Nature of Rock Anticipated: Serpentinitized peridotite.

Site: MAR-ALT1S

Priority: Alternate

Position: 15.1167°N, 45.2667W°

Water Depth: 1650 mbsl (1661 mbrf)

Target Drilling Depth: 300 mbsf

Approved Maximum Penetration: 300 mbsf

Survey Coverage: None

Objective: Shallowest point in the region. Four dredge hauls from all sides of this mountain recovered peridotite. Part of the transverse ridge mountains, with a fairly flat top, it has the potential to be similar to Site 735, but for mantle drilling.

Drilling Program: Single bit penetration as deep as possible or 300 mbsf.

Logging Program: Two logging runs, triple combo and FMS-sonic if hole conditions permit.

Nature of Rock Anticipated: Serpentinized peridotite.

Site: MAR-ALT2S

Priority: Alternate

Position: 14.7226°N, 44.8922°W

Water Depth: 2075 mbsl (2086 mbrf)

Target Drilling Depth: 300 mbsf

Approved Maximum Penetration: 300 mbsf

Survey Coverage: MODE 98, Leg 1, dive 425

Objective: Location on the eastern limit of the axial valley exposing a fault surface of mylonitic peridotite. This site is on the flat-topped ridge above this fault surface, and drilling is likely to penetrate the footwall of the observed low-angle fault. This is also the farthest south site in the region from which peridotite has been sampled.

Drilling Program: Single bit penetration as deep as possible or 300 mbsf.

Logging Program: Two logging runs, triple combo and FMS-sonic if hole conditions permit.

Nature of Rock Anticipated: Serpentinized peridotite.

SCIENTIFIC PARTICIPANTS*

Co-Chief Scientist

Peter B. Kelemen

Department of Geology and Geophysics
Woods Hole Oceanographic Institution
Woods Hole MA 02543
USA
Internet: peterk@cliff.who.edu
Work: (508) 289-2956
Fax: (508) 457-2183

Co-Chief Scientist

Eiichi Kikawa

Japan Marine Science and Technology Center
Washington DC Office
1133 21st Street Northwest
Suite 400
Washington DC 20036
USA
Internet: kikawa@jamstec.org
Work: (202) 872-0000
Fax: (202) 872-8300

Staff Scientist

D. Jay Miller

Ocean Drilling Program
Texas A&M University
1000 Discovery Drive
College Station TX 77845-9547
USA
Internet: miller@odpemail.tamu.edu
Work: (979) 845-2197
Fax: (979) 845-0876

Logging Staff Scientist

Anne C. M. Bartetzko

Angewandte Geophysik
Rheinisch-Westfälischen Technischen Hochschule
Aachen
RW Technische Hochschule
Lochnerstrasse 4-20
52056 Aachen6
Germany
Internet: A.Bartetzko@geophysik.rwth-aachen.de
Work: (49) 241-806773
Fax: (49) 241-8888-132

Logging Staff Scientist

Gerardo J. Iturrino

Lamont-Doherty Earth Observatory
of Columbia University
Borehole Research Group
Palisades NY 10964
USA
Internet: iturrino@ldeo.columbia.edu
Work: (914) 365-8656
Fax: (914) 365-3182

Schlumberger Engineer

Kerry Swain

Schlumberger Offshore Services
369 Tristar Drive
Webster TX 77598
USA
internet: swaink@webster.oilfield.slb.com
Work: (281) 480-2000
Fax: (281) 480-9550

Operations Manager

Michael A. Storms

Ocean Drilling Program
Texas A&M University
1000 Discovery Drive
College Station TX 77845-9547
USA
Internet: storms@odpemail.tamu.edu
Work: (979) 845-2101
Fax: (979) 845-2308

ODP Drilling Engineer

Richard Dixon

Ocean Drilling Program
Texas A&M University
1000 Discovery Drive
College Station TX 77845
USA
Internet: dixon@odpemail.tamu.edu
Work: (979) 845-3207
Fax: (979) 845-2308

Laboratory Officer

Roy Davis

Ocean Drilling Program
Texas A&M University
1000 Discovery Drive
College Station TX 77845-9547
USA
Internet: davis@odpemail.tamu.edu
Work: (979) 845-2367
Fax: (979) 845-0876

Assistant Laboratory Officer

Chieh Peng

Ocean Drilling Program
Texas A&M University
1000 Discovery Drive
College Station TX 77845-9547
USA
Internet: peng@odpemail.tamu.edu
Work: (979) 845-0879
Fax: (979) 845-0876

*Staffing is incomplete and subject to change.

**Marine Laboratory Specialist: Yeoperson
Michiko Hitchcox**

Ocean Drilling Program
Texas A&M University
1000 Discovery Drive
College Station TX 77845-9547
USA
Internet: hitchcox@odpemail.tamu.edu
Work: (979) 845-2483
Fax: (979) 845-0876

**Marine Laboratory Specialist: Chemistry
Lisa Brandt**

Ocean Drilling Program
Texas A&M University
1000 Discovery Drive
College Station TX 77845
USA
Internet: imbrandt@students.wisc.edu
Work: (979) 845-3602
Fax: (979) 845-0876

**Marine Laboratory Specialist: Chemistry
Dennis Graham**

Ocean Drilling Program
Texas A&M University
1000 Discovery Drive
College Station TX 77845-9547
USA
Internet: graham@odpemail.tamu.edu
Work: (979) 845-3602
Fax: (979) 845-0876

**Marine Laboratory Specialist: Core
Eric Jackson**

Ocean Drilling Program
Texas A&M University
1000 Discovery Drive
College Station TX 77845-9547
USA
Internet:
Work: (979) 845-3602
Fax: (979) 845-0876

**Marine Laboratory Specialist: Curator
Paula Weiss**

Ocean Drilling Program
Texas A&M University
1000 Discovery Drive
College Station TX 77845-9547
USA
Internet: pweiss@qwest.net
Work: (979) 845-3602
Fax: (979) 845-0876

**Marine Laboratory Specialist: Downhole Tools/
Thin Sections**

Ted Gustafson
Ocean Drilling Program
Texas A&M University
1000 Discovery Drive
College Station TX 77845-9547
USA
Internet: gustafson@odpemail.tamu.edu
Work: (979) 845-3602
Fax: (979) 845-0876

**Marine Laboratory Specialist: Paleomagnetism
Scott Herman**

Ocean Drilling Program
Texas A&M University
1000 Discovery Drive
College Station TX 77845-9547
USA
Internet: hermanscott@hotmail.com
Work: (979) 845-3602
Fax: (979) 845-0876

**Marine Laboratory Specialist: Photographer
Cyndi J. Prince**

Ocean Drilling Program
Texas A&M University
1000 Discovery Drive
College Station TX 77845-9547
USA
Internet: prince@odpemail.tamu.edu
Work: (979) 845-2480
Fax: (979) 845-0876

**Marine Laboratory Specialist: Physical Properties
William S. Hammon III**

Ocean Drilling Program
Texas A&M University
1000 Discovery Drive
College Station TX 77845-9547
USA
Internet: shammon@odpemail.tamu.edu
Work: (979) 845-3602
Fax: (979) 845-0876

**Marine Laboratory Specialist: Underway Geophysics
Lisa K. Crowder**

Ocean Drilling Program
Texas A&M University
1000 Discovery Drive
College Station TX 77845-9547
USA
Internet: crowder@odpemail.tamu.edu
Work: (979) 845-7716
Fax: (979) 845-0876

Marine Electronics Specialist

Randy W. Gjesvold

Ocean Drilling Program

Texas A&M University

1000 Discovery Drive

College Station TX 77845-9547

USA

Internet: gjesvol@linknet.kitsap.lib.wa.us

Work: (979) 845-3602

Fax: (979) 845-0876

Marine Electronics Specialist

Michael Meiring

Ocean Drilling Program

Texas A&M University

1000 Discovery Drive

College Station TX 77845-9547

USA

Internet: kleinmeiring@yahoo.com

Work: (979) 845-3602

Fax: (979) 845-0876

Marine Computer Specialist

David Morley

Ocean Drilling Program

Texas A&M University

1000 Discovery Drive

College Station TX 77845-9547

USA

Internet: morley@odpemail.tamu.edu

Work: (979) 862-4847

Fax: (979) 845-4857